Bioorganic Chemistry xxx (xxxx) xxxx

Contents lists available at ScienceDirect

Bioorganic Chemistry

journal homepage: www.elsevier.com/locate/bioorg

The synthetic flavanone 6-methoxy-2-(naphthalen-1-yl)chroman-4-one induces apoptosis and activation of the MAPK pathway in human U-937 leukaemia cells

Ester Saavedra[a], Henoc Del Rosario[a], Ignacio Brouard[b], Judith Hernández-Garcés[c], Celina García[c], José Quintana[a], Francisco Estévez[a,*]

[a] Departamento de Bioquímica y Biología Molecular, Unidad Asociada al Consejo Superior de Investigaciones Científicas (CSIC), Instituto Universitario de Investigaciones Biomédicas y Sanitarias (IUIBS), Universidad de las Palmas de Gran Canaria, Spain
[b] Instituto de Productos Naturales y Agrobiología, CSIC, La Laguna, Tenerife, Spain
[c] Instituto Universitario de Bio-orgánica AG, Departamento de Química Orgánica, Universidad de La Laguna, Tenerife, Spain

ARTICLE INFO

Keywords:
Apoptosis
Structure-activity relationship
Caspase
Cell cycle
Cytotoxicity
Flavanone

ABSTRACT

Synthetic flavonoids containing a naphthalene ring have attracted attention as potential cytotoxic compounds. Here, we synthesized ten chalcones and their corresponding flavanones and evaluated their antiproliferative activity against the human tumour cell line U-937. This series of chalcone derivatives was characterized by the presence of a naphthalene ring which was kept unaltered- and attached to the β carbon of the 1-phenyl-2-propen-1-one framework. The structure-activity relationship of these chalcone derivatives and their corresponding cyclic compounds was investigated by the introduction of different substituents (methyl, methoxy, benzyloxy, chlorine) or by varying the position of the methoxy or benzyloxy groups on the A ring. The results revealed that both the chalcone containing the methoxy group at 5′ position of the A ring as well as its corresponding flavanone [6-methoxy-2-(naphthalen-1-yl)chroman-4-one] were the most cytotoxic compounds, with IC_{50} values of 2.8 ± 0.2 and 1.3 ± 0.2 μM, respectively, against U-937 cells. This synthetic flavanone was as cytotoxic as the antitumor etoposide in U-937 cells and displayed strong cytotoxicity against additional human leukaemia cell lines, including HL-60, MOLT-3 and NALM-6. Human peripheral blood mononuclear cells were more resistant than leukaemia cells to the cytotoxic effects of the flavanone. Treatment of U-937 cells with this compound induced G_2-M cell cycle arrest, an increase in sub-G_1 ratio and annexin-V positive cells, mitochondrial cytochrome *c* release, caspase activation and poly(ADP-ribose)polymerase processing. Apoptosis induction triggered by this flavonoid was blocked by overexpression of the anti-apoptotic protein Bcl-2. This flavanone induces phosphorylation of p38 mitogen-activated protein kinases, extracellular-signal regulated kinases and c-*jun N*-terminal kinases/stress-activated protein kinases (JNK/SAPK) following different kinetics. Moreover, cell death was attenuated by the inhibition of mitogen-activated extracellular kinases and JNK/SAPK and was independent of reactive oxygen species generation.

1. Introduction

Cancer is the second most common cause of death among children aged 1 to 14 years in the United States and leukaemia accounts for 29% for all childhood cancers. Cancer survival has improved especially for hematopoietic and lymphoid malignancies due to improvements in treatment protocols, including the discovery of targeted therapies. The 5-year relative survival rate for all cancers combined improved from 58% during the mid-1970s to 83% during 2007 through 2013 for children. The lowest survival rate corresponds to acute myeloid leukaemia with a value of 65.1% between 2007 and 2013 [1]. In accordance with the GLOBOCAN estimates of incidence and mortality

Abbreviations: ERK, extracellular signal-regulated kinase; FL, 6-methoxy-2-(naphthalen-1-yl)chroman-4-one; IC_{50}, 50% inhibition of cell growth; JNK/SAPK, c-*jun N*-terminal kinases/stress-activated protein kinases; MAPK, mitogen-activated protein kinases; MEK, mitogen-activated extracellular kinases; MTT, 3-(4,5-dimethyl-2-thiazolyl)-2,5-diphenyl-2*H*-tetrazolium bromide; $p38^{MAPK}$, p38 mitogen-activated protein kinases; ROS, reactive oxygen species

* Corresponding author at: Departamento de Bioquímica y Biología Molecular, Universidad de Las Palmas de Gran Canaria, Paseo Blas Cabrera Felipe s/n, Las Palmas de Gran Canaria 35016, Spain.
E-mail address: francisco.estevez@ulpgc.es (F. Estévez).

https://doi.org/10.1016/j.bioorg.2019.103450
Received 14 June 2019; Received in revised form 19 September 2019; Accepted 14 November 2019

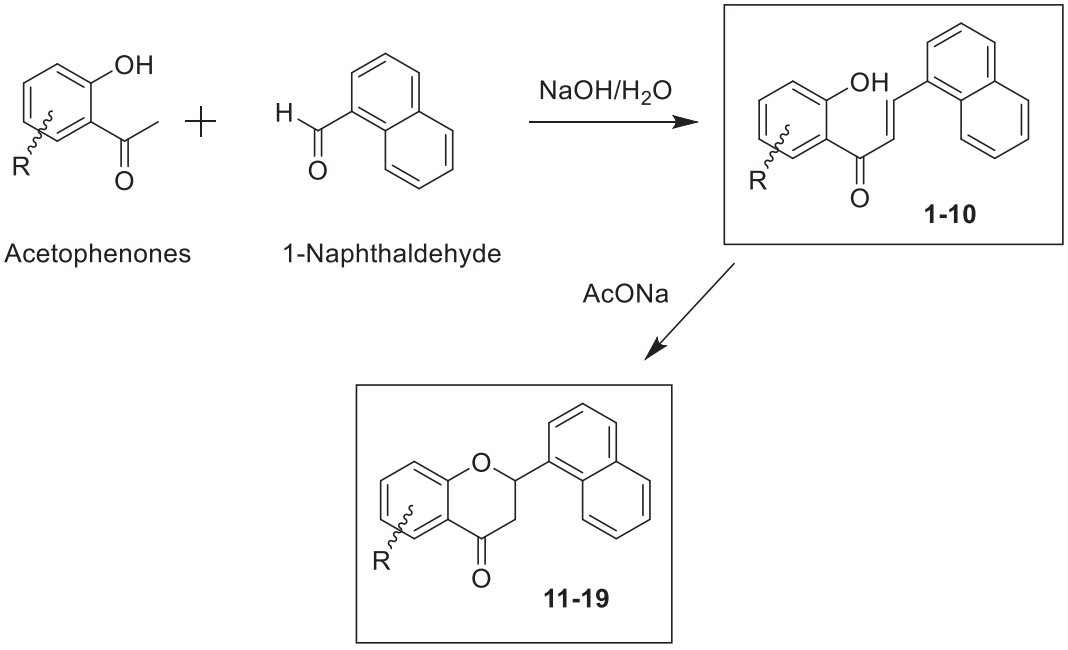

Scheme 1. Synthesis of chalcones and flavanones.

worldwide for 2018, the estimated numbers of new cases and deaths from leukaemia were 437,033 and 309,006, respectively, indicating that mortality rates for this disease are still very high [2], and providing an urgent need for improved treatments.

Natural products represent realistic options as potential cytotoxic compounds against cancer cells [3]. Flavonoids are secondary polyphenolic metabolites present in almost all plants and the human diet. These compounds exhibit a wide spectrum of pharmacological properties that have been recently reviewed [4,5]. Flavonoids are able to interfere in all phases of cancer progression by modulating key proteins involved in proliferation, differentiation, apoptosis, angiogenesis, metastasis and reverse multidrug resistance process. Apoptosis is a form of regulated cell death which results in destruction of target cell with minimal inflammatory response. Essential executioners of apoptosis are the caspases, a family of cysteine proteases which are expressed in cells as inactive zymogens known as procaspases. These enzymes predominantly cleave their substrates on the C-terminal side of aspartate. Proteolytic cleavage leads to important changes in cell morphology such as membrane blebbing, DNA fragmentation, phosphatidylserine exposure at the cell surface, and formation of apoptotic vesicles. Two main apoptotic pathways have been described, the mitochondrial and the extrinsic pathways [6]. The mitochondrial or intrinsic pathway is initiated by perturbations of the intracellular or extracellular microenvironment, demarcated by mitochondrial outer membrane permeabilization and precipitated mainly by caspase-3. The extrinsic pathway is initiated by perturbations of the extracellular microenvironment that are detected by plasma membrane receptors (propagated by caspase-8 and precipitated by executioner caspases, mainly caspase-3).

It is well established that mutual molecular recognition of host and guest depends on non-covalent interactions (H-bonding, stacking interactions, cation-π interactions, ionic interactions and hydrophobic interactions) which are the basis of the functional properties of most molecules. Inter and intramolecular interactions involving aromatic ring systems are key processes in chemical and biological recognition and knowledge of these helps explain and predict the functionality of different structures.

Interactions between aromatic platforms and sugar and aminoacid residues play a crucial role in determining the specificity of drug-receptor interaction processes. The planarity of the aromatic systems together with their polarizability and their multipolar moment are properties that illustrate the capacity of these systems to form functional complexes [7–9]. In particular, recent studies using small molecules carrying naphthalene groups describe the interaction of such a ring system with a hydrophobic pocket located in the Ras oncogene as causing the inhibition of that oncogene. Naphthalene also has the ability to generate strong π-π stacking interactions, providing high affinity ligands for more than one type of receptor, and making it a privileged scaffold. These findings suggest that the naphthalene ring could become a propitious building block for the development of new therapeutic agents [10].

Naphthalene-based chalcones, in which one of the aryl rings is replaced by naphthalene, have been explored as potential anticancer agents. The aim of this study was to synthesize a series of chalcone derivatives and their corresponding cyclic compounds containing a naphthalene ring to explore the effect of different substituents (methyl, methoxy, benzyloxy, chlorine) or changes in the position of the methoxy or benzyloxy groups on the phenyl ring on cytotoxicity against the human tumour U-937 cells. This cell line was selected as it is the most frequently used cell line in biomedical research for the study of neoplasia and therapeutics and has made important contributions to the disciplines of cancer, hematology, and immunology [11,12]. In addition, we investigated the signal transduction pathways of cell death triggered by one of the most cytotoxic compounds, the flavanone 6-methoxy-2-(naphthalen-1-yl)chroman-4-one (FL).

2. Results

2.1. Chemistry

In the present study, we explored the cytotoxic effects of a collection of 19 chalcones and flavanones containing a naphthalene core against human U-937 leukaemia cells. The chalcones (**1–10**) were prepared by a standard aldolic condensation procedure involving pH > 12 conditions. The aldolic condensation is one of the most versatile of organic chemical reactions because of its ability to use small molecules in the synthesis of larger ones under Claisen-Schmidt conditions. If this reaction is performed at lower pH (9–10) a reversible interconversion between the chalcone and its constitutional isomer flavanone is observed depending on the range of pH and on the substitution on the A ring [13]. The flavanones (**11–19**) were subsequently synthesized by

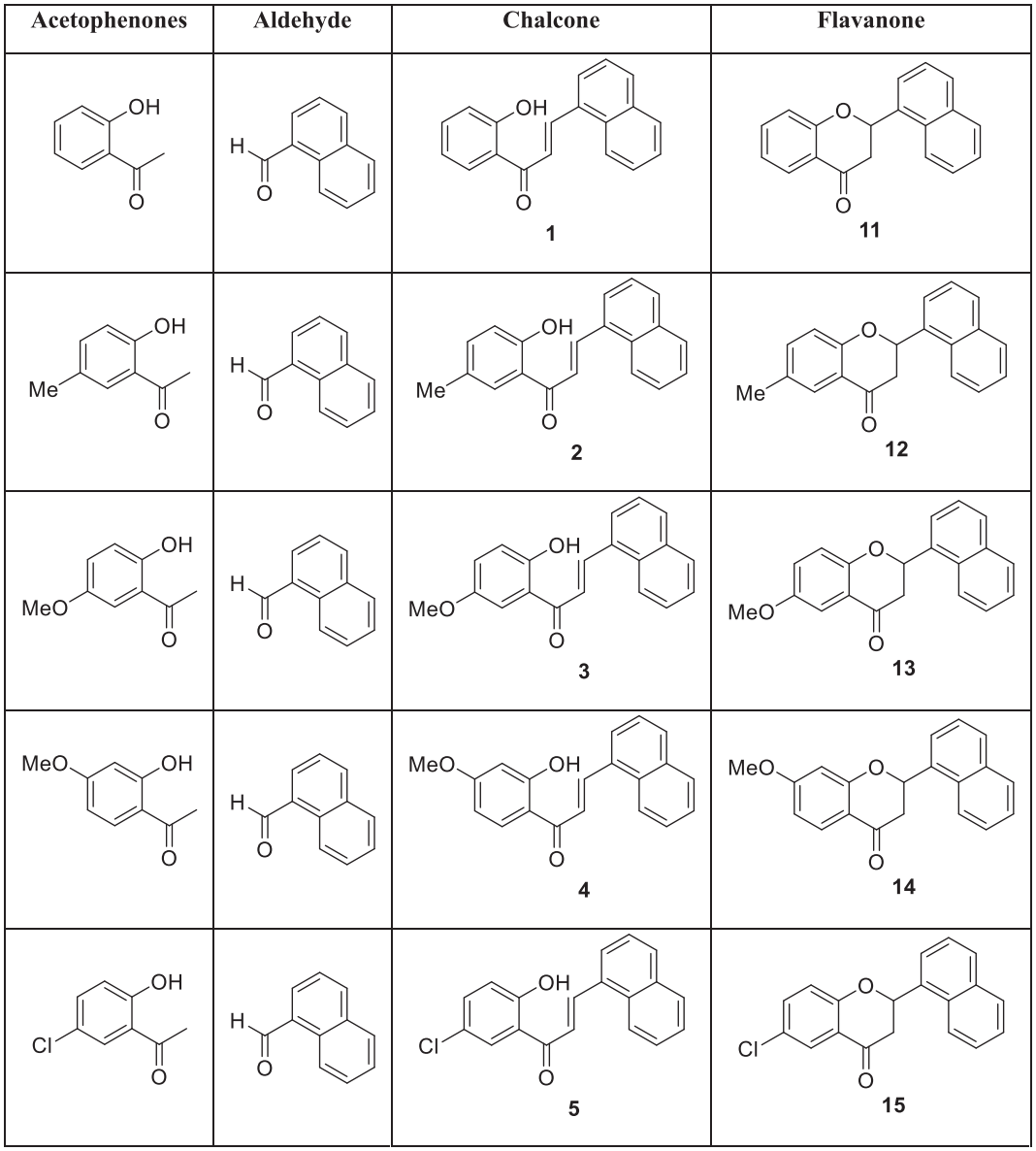

Scheme 2. Acetophenone derivatives and 1-naphthaldehyde used in the synthesis of the chalcones (**1–10**) and flavanones (**11–19**).

cyclization reactions of the above-mentioned chalcones in the presence of an excess of sodium acetate under reflux (Scheme 1). In the particular case of chalcone **10**, it was not possible to isolate the desired flavanone. Chalcones (**1–10**) and their corresponding flavanones were designed to contain one or two substituents in the A ring (Scheme 2).

2.2. Biology

2.2.1. Screening of synthetic flavonoids. The synthetic 6-methoxy-2-(naphthalen-1-yl)chroman-4-one (FL) inhibits the viability of human leukaemia cells

The SARs (structure-activity relationship) of naphthalene-based chalcones and their corresponding flavanones were investigated by varying the substituent on the A ring or the location of the methoxy and/or benzyloxy groups at the 4′ or 5′ position on the A ring. In this series of naphthalene-chalcones we maintained the naphthyl ring attached to the β carbon of the 2-propen-1-one system and added various substituents (hydrogen, methyl, chlorine, methoxy or benzylxoxy) at the 5′ position on the phenyl ring. In addition, we included another chlorine atom or another benzyloxy group and changed the position of the methoxy or the benzyloxy group at the 6′ position. To this end, U-937 cells were treated with increasing concentrations of each compound and the IC_{50} values (the concentration that induces a 50% inhibition of cell growth) were determined by the MTT assay.

The results indicated that the introduction of a methoxy group at position 5′ on the A ring (chalcone **3**) or at position 6 in the A ring of the corresponding flavanone (flavanone **13**) led to a significant improvement in cytotoxic activity, both in chalcones [(IC_{50} = 9.7 ± 2.0 μM for chalcone **1** vs IC_{50} = 2.8 ± 0.2 μM for chalcone **3**); 3.5-fold increase in cytotoxicity] and flavanones [(IC_{50} = 10.4 ± 3.1 μM for flavanone **11** vs. IC_{50} = 1.3 ± 0.2 μM for flavanone **13**); 8-fold increase in cytotoxicity]. In contrast, the introduction of the methyl group or an atom of chlorine in this position appears to be irrelevant in determining cytotoxicity against U-937 cells. The presence of an additional chlorine atom at position 3′ did not change the cytotoxicity of the chalcone (**8**, IC_{50} = 13.4 ± 7.2 μM) or the flavanone (**18**, IC_{50} = 8.2 ± 3.0 μM) skeleton. Moreover, the introduction of a methoxy group at position 4′ of the chalcone skeleton (chalcone **4**) did not enhance the potency against cell growth inhibition compared with chalcone **1**.

The introduction of one or two benzyloxy groups at the 4′ and 5′

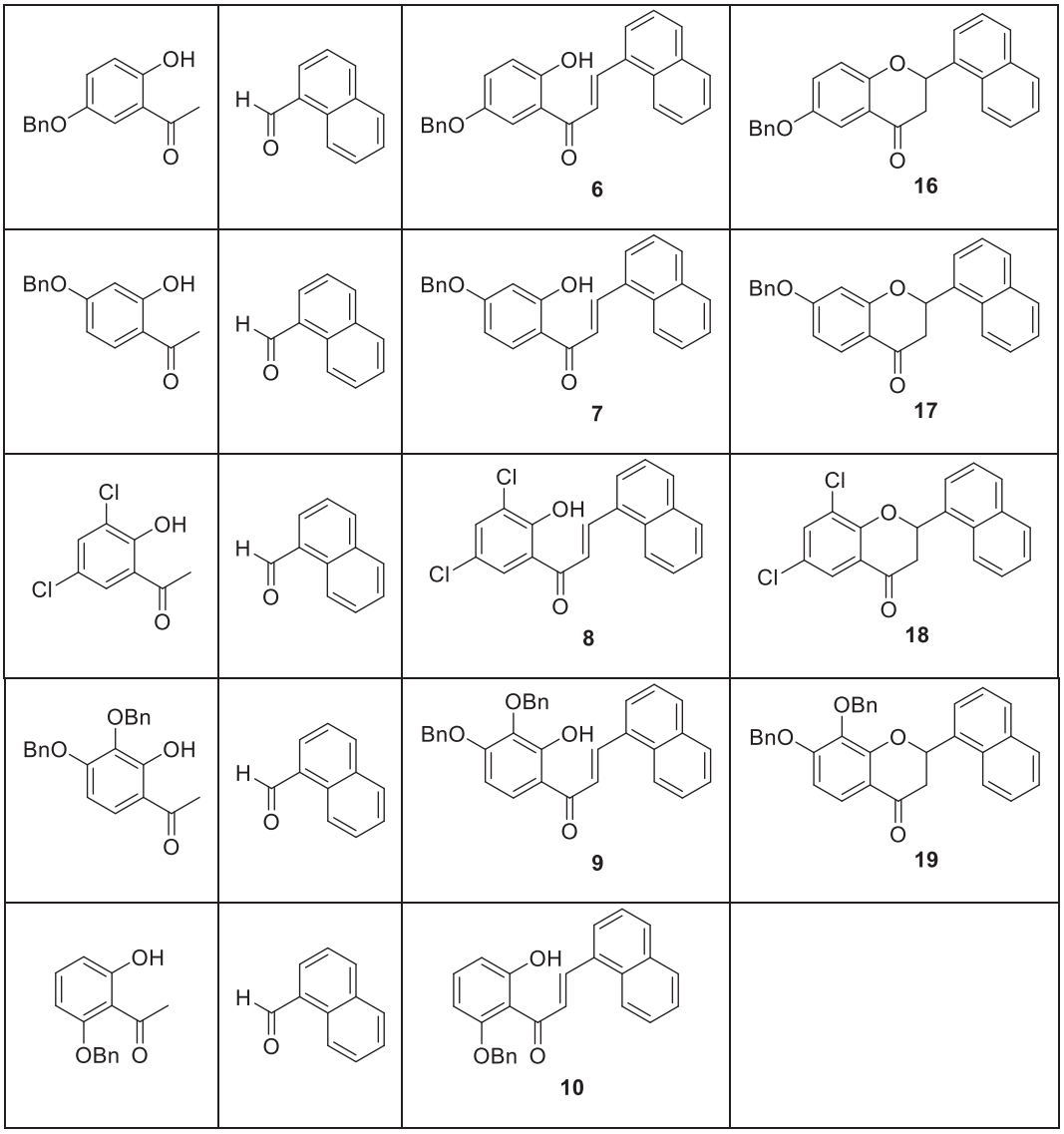

Scheme 2. (*continued*)

positions on the A ring of chalcones or at positions C6 or C7 and C8 of flavanones significantly decreased cytotoxic activity (chalcones: IC_{50} > 30 μM for **7** and **9** and IC_{50} = 20.3 ± 9.0 μM for **6**, flavanones: IC_{50} > 30 μM for **17**, **16** and **19**). The bulky groups on the A ring appear to interfere with the cytotoxic activity and might be explained for their low solubility due to the presence of the aromatic rings and exacerbated by the naphthyl group.

Since there are no large differences in cytotoxic activity between chalcones and flavanones, these results suggest that the major determinant of cytotoxicity is the presence and the position of a methoxy group on the A ring, and that the most cytotoxic compounds were the chalcone **3** and the flavanone **13** with IC_{50} values of 2.8 ± 0.2 and 1.3 ± 0.2 μM, respectively for U-937 cells (Table 1).

Since flavanone **13** [6-methoxy-2-(naphthalen-1-yl)chroman-4-one, FL] was found to be one of the most cytotoxic compounds, it was selected for further experiments. Comparison with additional human leukaemia cells revealed that FL displays strong cytotoxic properties against three human leukaemia cell lines, including the human acute myeloid leukaemia HL-60, the human B cell precursor leukaemia NALM-6 and the acute lymphoblastic leukaemia MOLT-3, with IC_{50} values between 1 and 3 μM (Table 2). For comparison, the standard antitumor agent etoposide was included as a positive control for U-937

Table 1
Effects of flavonoids on the growth of human tumour cell line U-937.

Chalcone	**1**	**2**	**3**	**4**	**5**	**6**	**7**	**8**	**9**	**10**
IC_{50} (μM)	9.7 ± 2.0	8.3 ± 2.2	2.8 ± 0.2	8.5 ± 0.9	7.5 ± 1.6	20.3 ± 9.0	> 30	13.4 ± 7.2	> 30	12.6 ± 3.9
Flavanone	**11**	**12**	**13**	**14**	**15**	**16**	**17**	**18**	**19**	
IC_{50} (μM)	10.4 ± 3.1	22.6 ± 3.0	1.3 ± 0.2	15.3 ± 5.0	5.7 ± 2.1	> 30	> 30	8.2 ± 3.0	> 30	

Cells were cultured for 72 h in presence of the indicated compounds and the IC_{50} values were calculated as described in the Experimental Section. The data shown represent the mean ± SEM of 3 independent experiments with three determinations in each.

Table 2
Effects of FL on cell viability of human leukaemia cell lines.

IC_{50} (μM)		
HL-60	NALM-6	MOLT-3
2.0 ± 1.5	3.1 ± 1.0	1.1 ± 0.2

Cells were cultured for 72 h and IC_{50} values were calculated as described in the Experimental Section. Representable values are means ± SE from 3 to 5 independent experiments with determinations performed in triplicate.

(IC_{50} = 1.2 ± 0.2 μM), HL-60 (IC_{50} = 0.4 ± 0.1 μM) and MOLT-3 (IC_{50} = 0.2 ± 0.1 μM).

Treatment of the human histiocytic lymphoma U-937 cells with this flavanone resulted in a concentration-dependent inhibition of cell viability (Fig. 1A), induced significant morphological changes and caused an important reduction in the number of cells (Fig. 1B). Studies using the trypan blue exclusion method showed that FL displays cytotoxicity but it is not cytostatic against U-937 cells. Fig. 1C–E show the number of total cells, live cells and the percentage of live cells after treatment with 10 μM FL during increasing periods of time. In addition, quiescent and proliferating peripheral blood mononuclear cells isolated from healthy volunteers were more resistant to the cytotoxic effects of FL than human leukaemia U-937 cells (Fig. 1F). These results indicate that FL exhibits strong cytotoxic properties against leukaemia cells but has only weak cytotoxic effects against peripheral blood mononuclear cells (PBMCs).

2.2.2. FL induces G_2-M arrest and apoptosis in human myeloid leukaemia cells

To determine whether the effects of FL on cell viability were due to alterations in cell cycle progression, cells were incubated with increasing concentrations for different time periods (6–24 h), stained with propidium iodide and analyzed by flow cytometry. As shown (Table 3, Fig. 2A) an exposure at a concentration as low as 3 μM FL caused a significant G_2-M arrest at the expense of G_1 phase cell population which was evident after 6 h of treatment. The percentage of cells in G_2-M phase increased from ~21% in control cells to ~36% after treatment with FL for 12 h. Moreover, the percentage of hypodiploid cells (i.e.

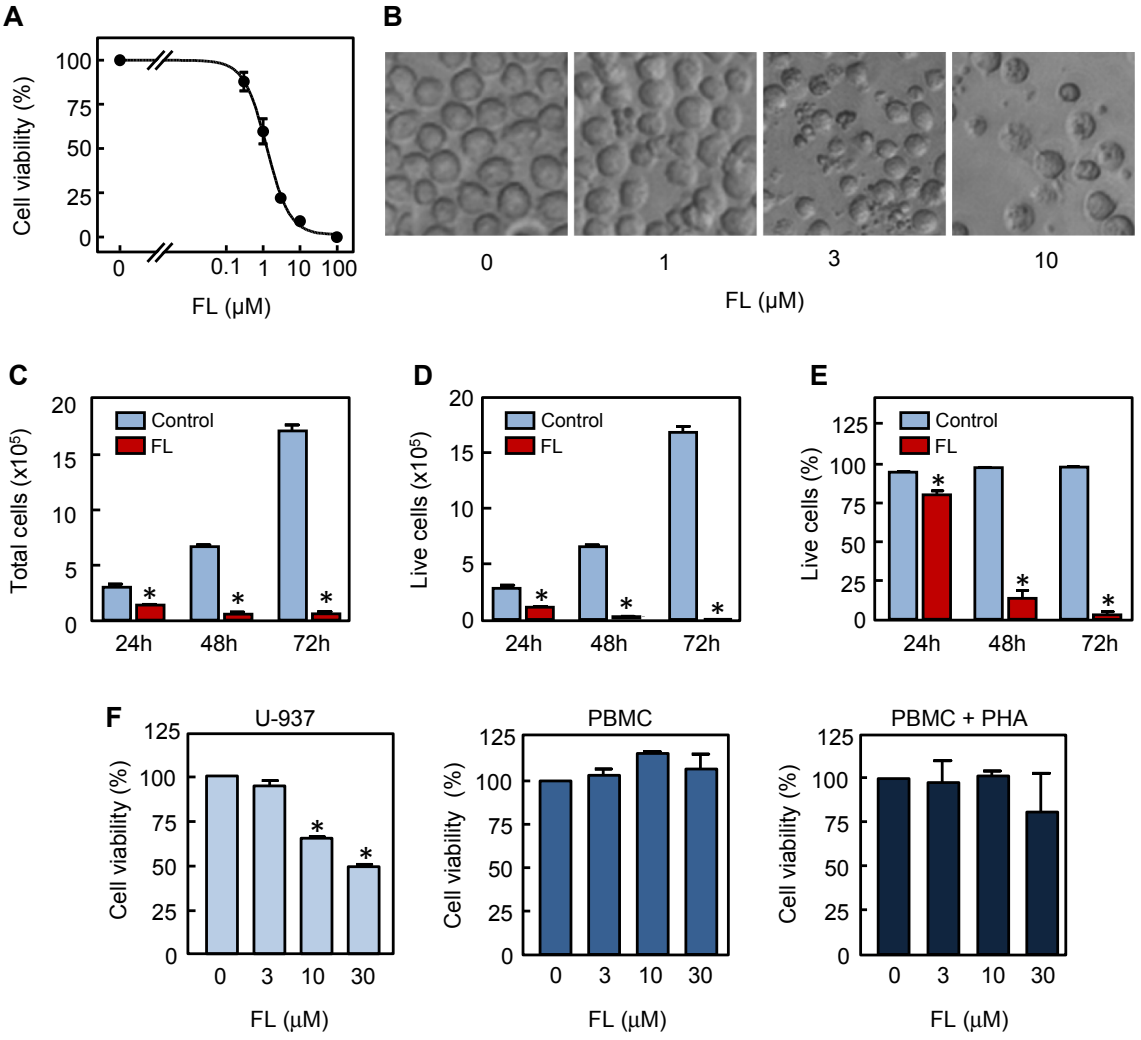

Fig. 1. FL is cytotoxic against human leukaemia U-937 cells but not against peripheral blood mononuclear cells. (A) Dose-response study of FL on U-937 cells viability. Cells were incubated with increasing concentrations of FL for 72 h, and thereafter cell viability was determined by the MTT assay. (B) Photomicrographs of morphological changes visualized with inverted phase contrast microscopy after treatment with the indicated concentrations of FL for 24 h. (C–E) Time-course of FL-mediated cell death. Cells were incubated with FL (10 μM) for the indicated times and the number of total cells (C), live cells (D) and the percentage of live cells were determined by the trypan blue exclusion method using a TC10 counter (Bio-Rad, Hercules, CA). (F) Differential effects of FL on cell viability of U-937 and quiescent and phytohemagglutinine (PHA)-activated healthy human peripheral blood mononuclear cells (PBMC). Cells were incubated in the presence of the specified concentrations of FL for 24 h and thereafter cell viability was determined by the MTT assay. Values represent means ± SE of two independent experiments each performed in triplicate. *$P < 0.05$, significantly different from the untreated control.

Table 3
Effect of FL on cell cycle phase distribution of U-937 leukaemia cells.

	(μM)	% Sub-G_1	%G_1	%S	%G_2-M
6 h	0	1.4 ± 0.2	52.5 ± 2.2	24.4 ± 1.0	21.7 ± 3.3
	1	2.9 ± 0.2	45.6 ± 1.0	26.7 ± 0.4	24.7 ± 1.1
	3	4.2 ± 0.4	29.0 ± 1.1*	33.4 ± 0.4*	33.3 ± 1.4*
	10	3.3 ± 0.3	19.8 ± 0.7*	34.5 ± 1.2*	42.3 ± 2.0*
12 h	0	0.9 ± 0.1	51.5 ± 0.8	26.5 ± 0.6	21.0 ± 0.9
	1	1.5 ± 0.2	50.6 ± 0.4	24.7 ± 0.1	23.1 ± 0.4
	3	8.0 ± 1.8*	29.0 ± 1.5*	27.4 ± 3.4	35.6 ± 3.7*
	10	7.4 ± 0.5*	7.3 ± 0.5*	31.7 ± 1.2*	53.6 ± 2.1*
24 h	0	1.4 ± 0.1	55.6 ± 0.2	27.6 ± 0.9	15.8 ± 0.9
	1	2.6 ± 0.3	51.0 ± 0.6	29.4 ± 0.1	17.0 ± 0.4*
	3	25.9 ± 3.4*	17.0 ± 0.6*	45.8 ± 2.6*	11.1 ± 1.9*
	10	39.2 ± 9.2*	17.3 ± 0.6*	24.5 ± 14	18.6 ± 4.9

Cells were cultured with the four concentrations of FL (0, 1, 3, 10 μM) over three time periods (6, 12, 24 h) and the percentages of cells in the four phases of the cell cycle (%Sub-G_1, %G_1, %S, %G_2-M) were determined by flow cytometry. The values are means ± S.E. of two independent experiments with three determinations in each. Asterisks indicate a significant difference ($P < 0.05$) compared with the corresponding controls.

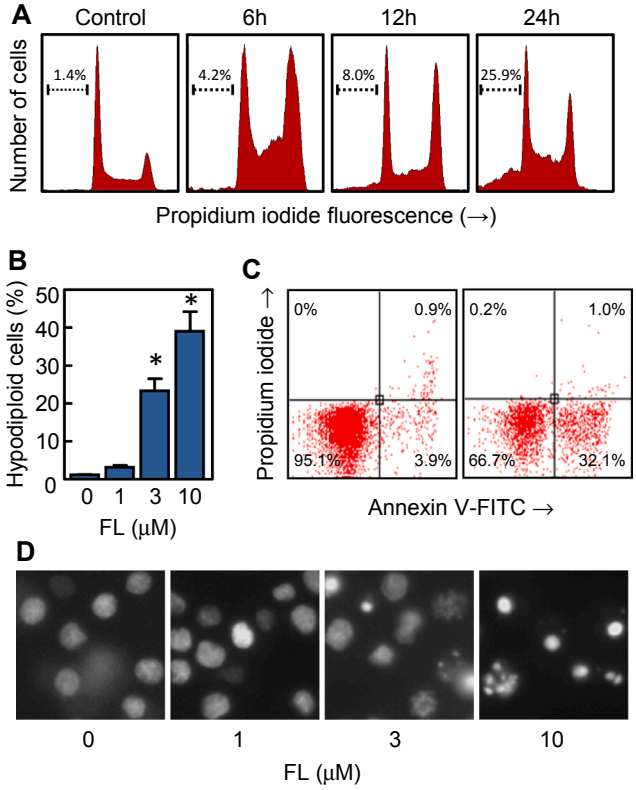

Fig. 2. Effect of FL on apoptosis on human myeloid leukaemia U-937 cells. (A) Cells were incubated in the presence/absence of 3 μM FL for the indicated times and subjected to flow cytometric analysis using propidium iodide labeling. The percentages of hypodiploid cells (apoptotic cells) are shown. (B) U-937 cells were incubated in the presence of the indicated concentrations of FL for 24 h and percentages of hypodiploid cells were quantified by flow cytometry. (C) Cells were treated with 10 μM FL for 24 h and subjected to flow cytometry analysis after annexin V-FITC and propidium iodide staining. (D) Photomicrographs of representative fields of U-937 cells stained with Hoechst 33,258 to evaluate nuclear chromatin condensation after treatment with the specified concentrations of FL for 24 h.

sub-G_1 fraction) increased about 18-fold in FL-treated U-937 compared with control cells after 24 h (Fig. 2A).

Maximal levels of apoptotic cells (approximately 30-fold increase with respect to control) were observed at 24 h with 10 μM FL in U-937 (Table 3, Fig. 2B). FL treatment also led to the exposure of phosphatidylserine on the outside of the plasma membrane as detected by Annexin V-FITC staining in U-937 cells (Fig. 2C). In addition, fluorescence microscopy experiments clearly demonstrate increases in condensed and fragmented chromatin, which is typical of apoptotic cells in U-937 (Fig. 2D). Taken together, these results indicate that FL induces cell cycle arrest in the G_2-M phase and apoptosis on human myeloid leukaemia U-937 cells.

2.2.3. Effects of FL on caspases- and PARP cleavage

To determine whether caspases were associated with the cell death triggered by FL, we examined the proteolytic processing of these proteases and PARP [poly(ADP-ribose) polymerase] cleavage. To this end, U-937 cells were treated with increasing concentrations of FL for 24 h, and caspases were determined by western blot (Fig. 3A). The results indicate that FL stimulates the cleavage of the main effector pro-caspase (pro-caspase-3) into 18–20 kDa fragments as well as the other executioner pro-caspases (pro-caspases-6 and -7). These effector caspases perform downstream execution of apoptosis. Interestingly, FL stimulated pro-caspase-4 processing as determined by a significant decrease in the zymogen levels. Processing of the main initiator caspases (pro-caspases-8 and -9) - involved in the extrinsic and the intrinsic apoptotic pathways - was detected by the visualization of the active 35–37 kDa fragment (pro-caspase-9) and a decrease of pro-caspase-8 levels. This flavanone also induced poly(ADP-ribose) polymerase (PARP) cleavage in accordance with caspase activation, generating the 85 kDa fragment. Protein loading was checked by reprobing the membranes with β-actin antibody.

To confirm that caspases processing correlates with activity, enzymatic activities of caspase-3-like protease (caspase-3/7), caspase-8 and caspase-9 were also investigated in extracts of U-937 cells treated with increasing concentrations of FL during 24 h. To this end, cell lysates were assayed for cleavage of the tetrapeptide substrates DEVD-*p*NA, IETD-*p*NA and LEHD-*p*NA as specific substrates for caspase-3/7, -8 and -9, respectively. As shown (Fig. 3B), dose-response experiments showed that a low concentration (1 μM) of FL was sufficient to induce caspases activation. A 2-fold increase in caspases-8 and -9 activities was observed in cells treated with 3 μM FL.

Confirmation that FL-triggered apoptosis requires the activation of caspases was carried out with cells pre-treated with the broad-spectrum caspase inhibitor z-VAD-fmk (100 μM). The results (Fig. 3C) showed that apoptosis was significantly suppressed in the presence of the inhibitor, which suggests that FL induces cytotoxicity by a caspase dependent mechanism. To determine which caspases are important in the mechanism of cell death triggered by this flavanone, we determined the effect of two sets of caspase inhibitors, including −CHO and –fmk derivatives. The −CHO derivatives included DEVD-CHO, LEVD-CHO, IETD-CHO and LEHD-CHO (all at 10 μM, except z-LEHD-CHO which was assayed at 50 μM, results not shown) and the –fmk derivatives included DEVD-fmk, IETD-fmk and LEHD-fmk (all at 50 μM, Fig. 3C). None of these inhibitors was able to decrease the percentage of hypodiploid cells induced by the flavanone. Fig. 3D shows the representative histograms of annexin V-FITC and propidium iodide-stained U-937 cells to confirm the effect of the pan-caspase inhibitor z-VAD-fmk. The lack of effect of the specific caspase inhibitors (z-DEVD-fmk, caspase-3/7 inhibitor; z-LEVD-CHO, caspase-4 inhibitor; z-IETD-fmk, caspase-8 inhibitor and z-LEHD-fmk, caspase-9 inhibitor) was also confirmed by flow cytometry after double staining with annexin V-FITC and propidium iodide (results not shown).

2.2.4. Effects of FL on mitochondrial proteins release and on Bcl-2 family members

Release of cytochrome *c* from mitochondria to cytosol is a central event in apoptotic signalling. To determine whether FL-induced apoptosis involves release of mitochondrial proteins, cytosolic preparations

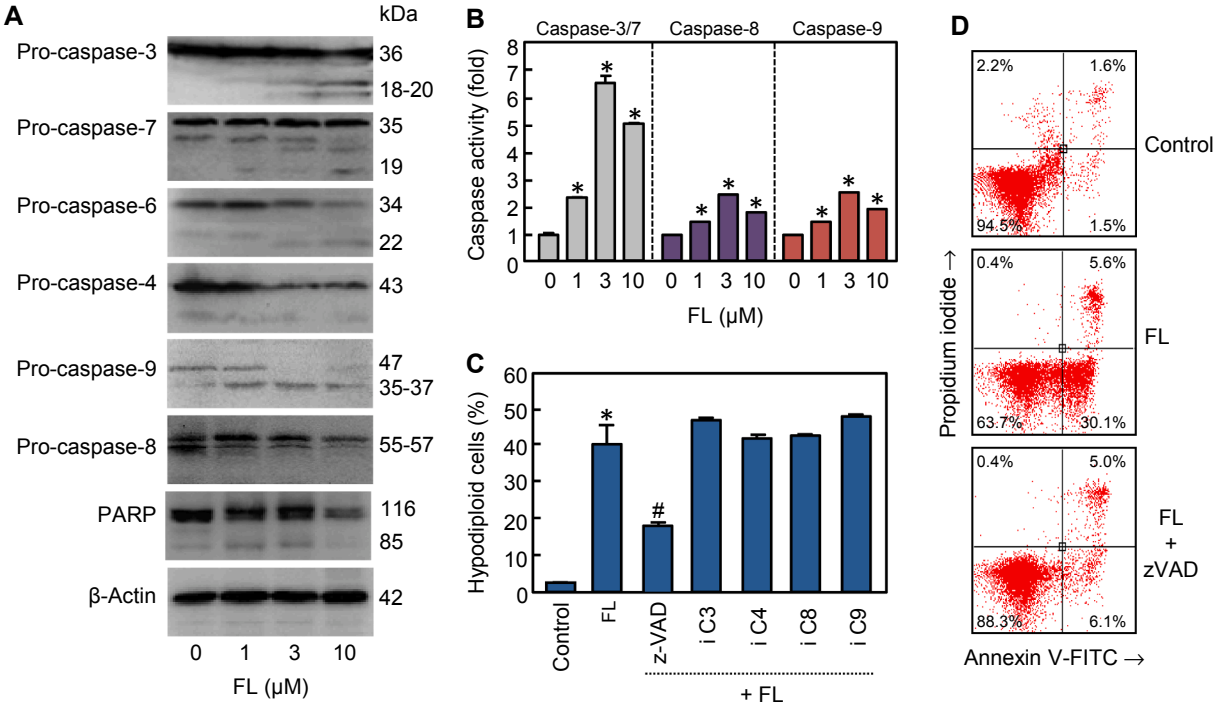

Fig. 3. Involvement of caspases in the mechanism of cell death triggered by FL in U-937 cells. (A) Immunoblotting for the cleavage of caspases and PARP after 24 h of treatment with the specified concentrations of FL. The protein β-actin was used as a loading control. (B) Activation of caspases in response to FL. Cells were incubated as above and cell lysates were assayed for caspase-3/7, caspase-8 and caspase-9 activities using the colorimetric substrates DEVD-*p*NA, IETD-*p*NA and LEHD-*p*NA, respectively. Results are expressed as the fold-increase in caspase activity compared with control. (C) Effect of cell-permeable caspase inhibitors on FL-induced apoptosis. Cells were incubated with 10 μM FL for 24 h, in presence or absence of the broad-spectrum caspase inhibitor z-VAD-fmk (z-VAD, 100 μM), the caspase-3/7 inhibitor z-DEVD-fmk (iC3, 50 μM), the caspase-4 inhibitor z-LEVD-CHO (iC4, 50 μM), the caspase-8 inhibitor z-IETD-fmk (iC8, 50 μM) and the caspase-9 inhibitor z-LEHD-fmk (iC9, 50 μM) and percentages of hypodiploid cells were quantified by flow cytometry. Bars represent the mean ± SE of two independent experiments each performed in triplicate. $^{*}P < 0.05$, significantly different from untreated control. $^{\#}P < 0.05$, significantly different from FL treatment alone. (D) Flow cytometry analysis of Annexin V-FITC and propidium iodide-stained cells after 24 h of treatment with 10 μM FL in absence or in presence of the pan-caspase inhibitor z-VAD-fmk (100 μM). Representative data from two independent experiments are presented.

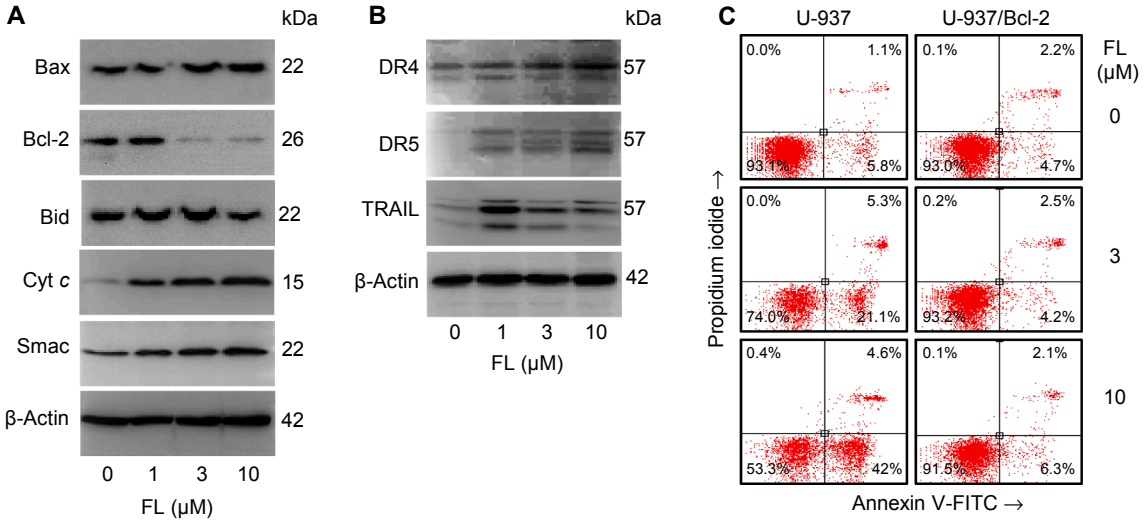

Fig. 4. Effect on Bcl-2 family proteins, release of mitochondrial proteins and expression of death receptors. (A) Cells were incubated with increasing concentrations of FL and the expression of Bcl-2 family members and release of cytochrome *c* and Smac/DIABLO were analyzed by western blot in U-937 cells. (B) Cells were treated as in (A) and expression of death receptors was detected by immunoblotting. β-Actin was used as a loading control. (C) U-937 and the cell line overexpressing Bcl-2, U-937/Bcl-2, were incubated with the specified concentrations of FL and apoptosis was determined by flow cytometry after double staining with annexin V-FITC and propidium iodide. The experiment was replicated twice.

were analyzed by immunoblotting of U-937 cells. The results showed a significant increase in the amount of cytochrome *c* in the cytosol in a concentration-dependent manner (Fig. 4A). There was also a concentration-dependent release of the mitochondrial apoptogenic factor Smac/DIABLO (second mitochondrial activator of caspases/Diablo IAP-binding mitochondrial protein).

We also investigated the expression of the Bcl-2 family proteins in FL-treated cells. The results revealed that flavanone induces

downregulation of Bcl-2 and a clear increase in Bax levels (Fig. 4A). In addition, there was a clear decrease in Bid protein, which is a substrate of caspase-8, indicating processing of this protein.

Since FL induces activation of caspase-8, it is possible that death receptors and/or their ligand might be involved in cell death. Therefore, we explored the effects of FL on the expression of DR4 (death receptor 4), DR5 (death receptor 5) and TRAIL (tumor necrosis factor-related apoptosis-inducing ligand) in U-937 cells. Cells were treated during 24 h and cell lysates were subjected to immunoblot analysis. As shown in Fig. 4B, FL up-regulates the expression of DR4, DR5 and TRAIL.

To clarify whether the anti-apoptotic protein Bcl-2 is involved in the activation of intrinsic pathway by FL treatment, we compared the effect on apoptosis in the U-937 cell line overexpressing human Bcl-2 protein (U-937/Bcl-2) and the parental U-937 cell line. As shown in Fig. 4C, Bcl-2 over-expression blocked apoptosis triggered by FL, suggesting that Bcl-2 is involved in FL-induced apoptosis.

2.2.5. FL activates MAPKs (mitogen-activated protein kinases) and cell death is independent on ROS (reactive oxygen species) generation

Whether FL induces the activation of the MAPK pathway or not was investigated because this signal transduction pathway plays a crucial role in cell fate. Incubation of U-937 cells with FL leads to a fast phosphorylation (0.5 h) of JNK/SAPK (*c*-jun *N*-terminal kinases/stress-activated protein kinases) and p38 ^{MAPK} while the activation of ERK1/2 (extracellular signal-regulated kinase) was not detected until 6 h (Fig. 5A). The activation of p38 ^{MAPK} decreased after 1 h, while the level of phosphorylated JNK/SAPK occurs in a biphasic manner. These results indicate that FL treatment of U-937 cells leads to activation of JNK/SAPK, p38^{MAPK} and ERK1/2 following different kinetics. To determine whether the phosphorylation of MAPKs plays a key role in FL-induced apoptosis, we examined the effects of p38^{MAPK}, JNK/SAPK, and mitogen-activated extracellular kinases 1/2 (MEK 1/2) inhibitors (Fig. 5B). Pretreatment of U-937 cells with the specific p38^{MAPK} inhibitor SB 203,580 (2 μM) did not affect the rate of FL-mediated apoptosis. These results suggest that activation of p38^{MAPK} is not involved in FL-induced cell death. Treatment of cells with U0126 or PD98059, inhibitors of MEK1/2, and with the JNK/SAPK inhibitor SP600125 significantly decreased FL-induced cell death. The percentage of apoptotic cells (hypodiploid cells) decreased from ~37% in FL-treated cells to 17% and 22% with U0126 and PD98059, respectively. The JNK/SAPK inhibitor attenuated FL-induced cell death from ~37% of apoptotic cells to 22% in the combination group (FL + SP600125). These results suggest that activation of ERK1/2 and JNK/SAPK is involved in FL–induced apoptosis.

Activation of the MAPK pathway can be mediated by the generation of reactive oxygen species (ROS). Hence the ability of FL to increase ROS levels was investigated using the fluorescent dye 2′, 7′-dichlorodihydrofluorescein diacetate after 1, 2 and 3 h of incubation, as well as the effect of different antioxidants [20 μM vitamin E, 2 mM trolox, 10 mM *N*-acetyl-L-cysteine, 0.5–1 μM diphenyleneiodonium chloride (a NADPH oxidase inhibitor); 500 units/ml catalase; 400 units/ml superoxide dismutase]. However, ROS were not generated at assayed times and the antioxidants did not reduce the cell death, either (results not shown). These results suggest that cell death is not dependent on ROS generation.

3. Discussion

Despite the potential of flavonoids in human medicine its clinical use is limited due to challenges associated with their effective use, including, among others, their pharmacokinetic and pharmacodynamic properties. Low solubility, poor oral absorption and extensive hepatic metabolism are responsible for the unfavorable pharmacokinetics of flavonoids. The modification of the flavonoid structure to generate new derivatives constitutes an important strategy to optimize their pharmacokinetic and pharmacodynamic properties. Previous studies have shown that methylation and/or the introduction of some lipophilic moieties in specific flavonoids significantly increase the potency and bioavailability and also enhance the stability and effectiveness by preventing chemical and metabolic hydrolysis [14–16].

In the present report, we attempted to find new potent antiproliferative molecules inspired by natural products. The results revealed that both the chalcone containing the methoxy group at 5′ position of the A ring as well as its corresponding flavanone were the most cytotoxic compounds, with IC_{50} values of 2.8 ± 0.2 and 1.3 ± 0.2 μM, respectively, against U-937 cells. This is the first time to date that the effects on cell viability and the mechanism involved in cell death induction have been investigated for this specific flavanone.

In a previous study, we showed that the synthetic chalcone 6′-benzyloxy-4-bromo-2′-hydroxychalcone is cytotoxic against seven human leukaemia cells and induces caspase-8- and reactive oxygen species-dependent apoptosis [17]. These results prompted us to design additional analogues of chalcone containing additional substituents other than halogen chalcones. When the 4-bromobenzyl group was replaced by a naphthyl group, the chalcone was unexpectedly cyclized

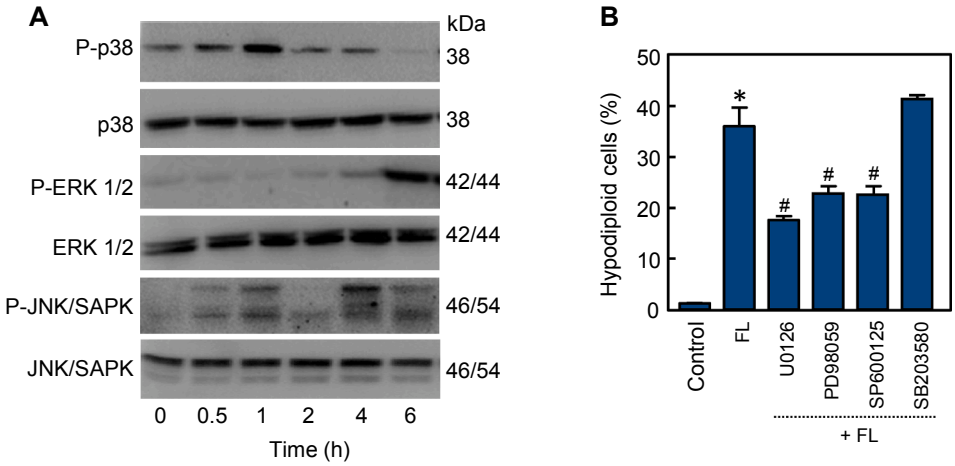

Fig. 5. Role of the MAPK pathway on FL-induced apoptosis in U-937 cells. (A) Representative Western blots show the time-dependent phosphorylation of p38 ^{MAPK}, ERK1/2 and JNK/SAPK by FL. Cells were incubated with 10 μM FL for the time periods shown. Protein extracts were prepared and analysed on Western blots probed with specific antibodies to ascertain the phosphorylation of MAPKs. Membranes were stripped and reprobed with total MAPK antibodies as loading controls. (B) Effect of MAPKs inhibitors on FL-induced cell death. Cells were preincubated with the MEK1/2 inhibitors U0126 (10 μM) and PD98059 (10 μM), the JNK/SAPK inhibitor SP600125 (10 μM) and the p38 ^{MAPK} inhibitor SB203580 (2 μM) for 1 h and then treated with FL. Apoptosis was quantified by flow cytometry as described in Materials and Methods. Bars represent the mean ± S.E. of three independent experiments each performed in triplicate. $^{*}P < 0.05$, significantly different from untreated control. $^{\#}P < 0.05$, significantly different from FL treatment alone.

to generate a flavanone (FL). This cyclic compound was found to have strong cytotoxic properties with IC_{50} values of approximately 2 μM against the four human leukaemia cell lines tested, including U-937, HL-60, NALM-6 and MOLT-3. Dose-response experiments revealed that U-937 cells were more sensitive to FL than quiescent and proliferating PBMC, as determined by the MTT assay. This flavanone is able to induce a fast cell cycle arrest at the G_2-M phase, starting at 6 h, and a delayed (later) increase in the percentage of hypodiploid cells. The arrest of cells in the G_2-M phase of the cell cycle by FL could be explained by microtubule formation or by changes in the expression and/or activity of G_2-M cell cycle regulators. Previous studies have shown that some flavonoids exert their anti-proliferative activity by targeting microtubules through tubulin binding [18] and we have reported that some naturally occurring and synthetic cytotoxic flavonoids block tubulin polymerization [19–21]. Further studies are needed to determine the effect of FL on tubulin polymerization and on G_2-M cell cycle regulators such as the cyclin-dependent kinases (Cdk) inhibitor $p21^{Cip1/WAF1}$, Cdk1, Cdc25C phosphatase and B-type cyclin isoforms.

Our results indicate that FL induces cell death by apoptosis, a process of programmed cell death that can occur with or without activation of caspases, but in this case cell death was dependent on caspases since the pan-caspase inhibitor z-VAD-fmk was able to significantly reduce both the percentage of hypodiploid cells and the percentage of annexin V-FITC positive cells. Our results showed that the flavanone induces the activation and processing of multiple caspases in U-937 cells. Caspase-6 which is believed to be an effector caspase that is activated downstream of caspase-3 and -7 in apoptosome-mediated apoptosis [22] and the effector caspase-7 which is substrate for initiator caspases in extrinsic or intrinsic apoptotic pathways were also processed. However, the specific caspase inhibitors against caspase-3/7, -4, -8 and -9 were unable to block the cell death. This raises the possibility that other specific caspases such as caspase-6 and/or additional pathways may play a key role in the mechanism of cell death. The potential involvement of caspase-6 is supported by recent data which indicate that caspase-6 may be involved in regulated cell death initiation [23–25].

The synthetic flavanone induced the release of mitochondrial apoptogenic proteins including cytochrome *c* and Smac/DIABLO. Cytochrome *c* in the cytosol binds to apoptotic peptidase activating factor 1 (Apaf-1) and pro-caspase-9 to form the apoptosome which is responsible for caspase-9 activation [26]. Smac/DIABLO in the cytosol precipitates apoptosis by binding with members of the inhibitor of apoptosis (IAP) protein family [27]. Although the specific caspase-9 inhibitor was unable to significantly block the cell death triggered by FL, the results seem to indicate that the intrinsic pathway, which is activated in response to cellular stress and is controlled by the Bcl-2 protein family, plays a key role. Treatment with the flavanone induced a strong downregulation of Bcl-2 protein in U-937. In addition, overexpression of Bcl-2 was able to block the cell death triggered by FL suggesting that Bcl-2 itself is a potential target in the mechanism of cell death. Furthermore, the Bax protein that promotes apoptosis was increased in U-937 cells, demonstrating that the ratio between proapoptotic and anti-apoptotic Bcl-2 members plays a major role in determining susceptibility of cells to apoptotic stimuli, as suggested by previous studies [28].

We found that FL also induces activation of caspase-8 which is involved in death receptor-mediated apoptosis. Caspase-8 cleaves Bid to a truncated form (tBid), which engages the mitochondrial pathway to amplify the apoptotic response. We did not observe a truncated form of Bid but the Western blot experiments revealed a clear decrease in Bid levels mainly at 10 μM FL in accordance with caspase-8 processing and activation. Since caspase-8 activation is mediated by ligand-binding and activation of the death-domain-containing tumor necrosis receptor superfamily we explored the involvement of death receptors. FL was found to effectively stimulate the expression of TRAIL, DR4 and DR5. Although further experiments are needed to determine whether FL is able to amplify the sensitivity to TRAIL these results are of potential importance because they demonstrate that FL is a death receptor inducer.

The mitogen activated protein kinase (MAPK) signalling pathway regulates the expression of a large number of proteins involved in the control of cell proliferation, differentiation and apoptosis. Activation of the MAPK signalling pathway is known to cause the transformation of normal cells to tumor phenotype [29,30]. Therefore, targeting any component in the MAPK signalling pathway has the potential to arrest tumor growth. Here we found that FL effectively activates the MAPK pathway and interestingly the activation of ERK1/2 and JNK/SAPK is involved in FL–induced apoptosis, since the MEK1/2 and JNK/SAPK inhibitors were able to block partially cell death. These results indicate a key role for the MAPK signalling cascade in the mechanism of cytotoxicity triggered by this flavanone. We have previously shown that betuletol 3-methyl ether, a naturally occurring flavonoid, induces the activation of mitogen-activated protein kinases. However, FL is a greater apoptotic inducer than betuletol 3-methyl ether and induces a fast phosphorylation of JNK/SAPK [31]. In addition, we have described that a flavonoid derivative, trifolin acetate, induces cell death in human leukaemia cells and that this was attenuated by MEK1/2 inhibition. However, this was different to the flavanone described here: the JNK/SAPK inhibitor SP600125 amplified cell death [32]. These results reveal that these flavonoid derivatives differentially modulate the MAPK pathways and could be used to enhance the cell death triggered by these specific compounds. An amplification of the cleavage of caspase-3 and PARP by JNK/SAPK inhibition has been also described in the mechanism of cell death triggered by the prenylated flavonoid daphnegiravone D in human hepatocellular carcinoma cells [33].

Future studies addressing the bioavailability – including the development of micro- and nanodelivery systems – as well as efficacy of *in vivo* concentrations of this specific compound are necessary to determine its potential beneficial effects for human health.

4. Conclusions

The SAR of naphthalene-based chalcones and their corresponding flavanones are displayed graphically in Fig. 6. The most relevant results are (i) some chalcones are more potent than their corresponding flavanones, while other chalcones show similar potency to flavanones, indicating that flexible structures are important in determining cytotoxicity; (ii) the introduction of a methoxy group at a specific position (position 5′ on the A ring in chalcone or at position 6 on the A ring of the corresponding flavanone) improved the cytotoxicity against U-937 cells and (iii) the introduction of a methyl group or an atom of chlorine appears to be irrelevant, while the presence of one or two benzyloxy groups on the A ring completely abrogates cytotoxicity, except for the 6′-benzyloxy derivative in the chalcone skeleton that showed a similar potency to the parent chalcone.

We show that the synthetic flavanone FL is cytotoxic against four human leukaemia cells but not against human peripheral blood mononuclear cells. FL-induced cytotoxicity (i) involves the activation and processing of the initiator (caspase-8 and -9) and the executioner caspases (caspases-3, -6 and -7); (ii) is attenuated by the pan-caspase inhibitor z-VAD-fmk; (iii) is associated with the phosphorylation of the mitogen-activated protein kinases ERK1/2, JNK/SAPK and $p38^{MAPK}$; and (iv) is reduced by the inhibition of MEK1/2 and JNK/SAPK. The IC_{50} values in human leukaemia cells were comparable with those obtained with the antitumor compound etoposide. The studies shown here open new avenues of research into the potential of this compound or derivatives in the development of new therapeutic strategies against leukaemia cells.

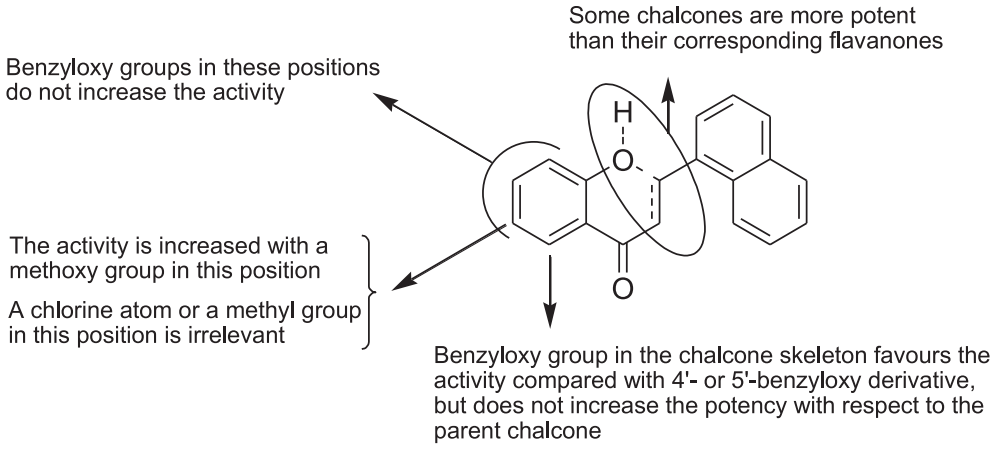

Fig. 6. Structure-activity relationship of naphthyl-chalcone/flavanone analogues.

5. Experimental

5.1. General method and reagents

^{1}H and ^{13}C NMR spectra were obtained on a Bruker model AMX-500 spectrometer with standard pulse sequences operating at 500 MHz in ^{1}H and 126 MHz in ^{13}C NMR. Chemical shifts (δ) are given in ppm upfield from tetramethylsilane as internal standard, and coupling constants (J) are reported in hertz. IR spectra were recorded using a Bruker model IFS-55 spectrophotometer. Melting points were determined on a Büchi B-540 apparatus and are un-corrected. EIMS and HREIMS were recorded on a Micromass model Autospec (70 eV) spectrometer. Column chromatography was carried out on silica gel 60 (Merck 230–400 mesh) and analytical thin layer chromatography (TLC) was performed using silica gel aluminum sheets. HPLC analyses were performed on a Waters 600 Controller using a Chiralcel OD-H column (iPrOH:hexane) and a Silica gel 100 Å LC column (250 × 4.6 mm – Hexane:ethyl acetate). Elemental analyses were performed on a Leco TruSpec Micro equipment. The purity of compounds used in biological testing was > 98%, as determined by elemental analysis or high-performance liquid chromatography. The inhibitors benzyloxycarbonyl-Val-Ala-Asp(OMe) fluoromethyl ketone (z-VAD-fmk), benzyloxycarbonyl-Asp(OMe)-Glu(O-Me)-Val-Asp(O-Me) fluoromethyl ketone (z-DEVD-fmk), benzyloxycarbonyl-Ile-Glu-Thr-Asp(OMe) fluoromethyl ketone (z-IETD-fmk), benzyloxycarbonyl-Leu-Glu-His-Asp(OMe) fluoromethyl ketone (z-LEHD-fmk), Ac-LEVD-CHO (*N*-acetyl-Leu-Glu-Val-Asp-CHO), PD98059, U0126, SP600125 and SB203580 were purchased from Sigma (Saint Louis, MO, USA). Acrylamide, bisacrylamide, ammonium persulfate and N,N,N′,N′-tetramethylethylenediamine were from Bio-Rad (Hercules, CA, USA). Antibodies for caspase-3, caspase-7, caspase-8 and caspase-9 were purchased from Stressgen-ENZO (Victoria, British Columbia, Canada). Anti-caspase-6 and anti-caspase-4 monoclonal antibodies were from Medical & Biological Laboratories (Nagoya, Japan). Monoclonal anti-β-Actin (clone AC-74) was purchased from Sigma (Saint Louis, MO, USA). Monoclonal anti-human Bcl-2 was from Santa Cruz Biotechnology (Santa Cruz, CA, USA). Polyclonal anti-human Bax and Bid antibodies and monoclonal anti-cytochrome *c* and poly(ADP-ribose) polymerase (PARP) antibodies were from BD Pharmingen (San Diego, CA, USA). Monoclonal antibody for Smac/DIABLO was from BD Transduction Laboratories. Anti-JNK/SAPK, anti-phospho-JNK/SAPK (T183/Y185), anti-p44/42 MAP kinase (ERK1/2), anti-phospho-p44/42 MAP kinase (T202/Y204), anti-p38MAPK and a phosphorylated form (T180/Y182) of p38MAPK were purchased from New England BioLabs (Cell Signaling Technology, Inc, Beverly, MA, USA). Secondary antibodies were from GE Healthcare Bio-Sciences AB (Little Chalfont, UK). PVDF membranes were from Millipore (Temecula, CA, USA). All other chemicals were obtained from Sigma (Saint Louis, MO, USA).

5.2. General procedure for the synthesis of chalcones (**1–10**)

A mixture of the acetophenone (5–10 mmol, 1 equiv.) and the corresponding aldehyde (1 equiv.) in EtOH (20–40 mL) was stirred at room temperature and a 50% aqueous solution of NaOH (5–8 mL) was added. The reaction mixture was stirred at room temperature until the starting materials had been consumed. HCl (10%) was then added until neutrality was reached. Precipitated chalcones were generally filtered and crystallized from MeOH although in some cases, the product was purified using column chromatography.

5.2.1. (E)-1-(2-hydroxyphenyl)-3-(naphthalen-1-yl)prop-2-en-1-one (**1**)

Yellow amorphous solid (65%). IR (cm^{-1}): 1694, 1640, 1607, 1581, 1566, 1491, 1472, 1462, 1439, 1365, 1342, 1304, 1278, 1209, 1159, 1072, 1024, 977, 901. ^{1}H NMR (500 MHz, $CDCl_3$): δ = 12.86 (s, 1H); 8.79 (d, J = 15.2 Hz, 1H); 8.29 (dd, J = 8.5, 1.0 Hz, 1H); 8.01–7.89 (m, 4H); 7.76 (d, J = 15.3 Hz, 1H); 7.62 (ddd, J = 8.4, 6.8, 1.5 Hz, 1H); 7.60–7.47 (m, 3H); 7.06 (dd, J = 8.4, 1.1 Hz, 1H); 6.97 (ddd, J = 8.2, 7.2, 1.2 Hz, 1H). ^{13}C NMR (126 MHz, $CDCl_3$): δ = 193.6, 163.7, 142.4, 136.5, 133.8, 132.1, 131.8, 131.2, 129.7, 128.8, 127.2, 126.4, 125.4, 125.3, 123.4, 122.8, 120.0, 118.9, 118.7. HRMS (ESI-FT-ICR) *m/z*: 297.0895 [M + Na]; calcd. for $C_{19}H_{14}NaO_2$: 297.0891.

5.2.2. (E)-1-(2-hydroxy-5-methoxyphenyl)-3-(naphthalen-1-yl)prop-2-en-1-one (**2**)

Orange crystalline solid (82%), mp 112–113 °C. IR (cm^{-1}): 1635, 1566, 1479, 1396, 1337, 1323, 1289, 1273, 1249, 1207, 1176, 1162, 1020, 1001, 979, 849. ^{1}H NMR (500 MHz, $CDCl_3$): δ = 12.68 (s, 1H); 8.77 (d, J = 15.2 Hz, 1H); 8.32–8.24 (m, 1H); 7.95 (t, J = 7.7 Hz, 2H); 7.93–7.86 (m, 1H); 7.75 (d, J = 15.3 Hz, 1H); 7.73 (s, 1H); 7.62 (ddd, J = 8.4, 6.8, 1.5 Hz, 1H); 7.59–7.50 (m, 2H); 7.34 (dd, J = 8.6, 2.2 Hz, 1H); 6.97 (d, J = 8.5 Hz, 1H); 2.36 (s, 3H). ^{13}C NMR (126 MHz, $CDCl_3$): δ = 193.5, 161.6, 142.1, 137.6, 133.8, 132.2, 131.8, 131.1, 129.4, 128.8, 128.0, 127.1, 126.4, 125.4, 125.3, 123.4, 122.9, 119.7, 118.4, 20.6. HRMS (ESI-FT-ICR) *m/z*: 311.1043 [M + Na]; calcd. for $C_{20}H_{16}NaO_2$: 311.1048.

5.2.3. (E)-1-(2-hydroxy-5-methoxyphenyl)-3-(naphthalen-1-yl)prop-2-en-1-one (**3**)

Orange crystalline solid (78%), mp 111–112 °C. IR (cm^{-1}):1644, 1581, 1566, 1495, 1417, 1346, 1271, 1188, 1166, 1048, 1017, 975, 960, 844. ^{1}H NMR (500 MHz, $CDCl_3$): δ = 12.42 (s, 1H); 8.78 (d, J = 15.2 Hz, 1H); 8.32–8.24 (m, 1H); 7.96 (d, J = 8.2 Hz, 1H);

7.94–7.88 (m, 2H); 7.69 (d, J = 15.2 Hz, 1H); 7.62 (ddd, J = 8.5, 6.8, 1.4 Hz, 1H); 7.60–7.51 (m, 2H); 7.40 (d, J = 3.0 Hz, 1H); 7.17 (dd, J = 9.1, 3.0 Hz, 1H); 7.01 (d, J = 9.1 Hz, 1H); 3.84 (s, 3H). ^{13}C NMR (126 MHz, $CDCl_3$): δ = 193.2, 158.1, 151.8, 142.5, 133.8, 132.1, 131.8, 131.2, 128.8, 127.2, 126.4, 125.4, 125.3, 124.1, 123.4, 122.9, 119.6, 119.4, 112.8, 56.1. HRMS (ESI-FT-ICR) *m/z*: 327.0999 [M + Na]; calcd. for $C_{20}H_{16}NaO_3$: 327.0997.

*5.2.4. (E)-1-(2-hydroxy-4-methoxyphenyl)-3-(naphthalen-1-yl)prop-2-en-1-one (**4**)*

Pale yellow crystalline solid (58%), mp 114–115 °C. IR (cm^{-1}): 1583, 1573, 1500, 1356, 1249, 1204, 1171, 1121, 1088, 1020, 1005, 958, 849, 828. ^{1}H NMR (500 MHz, $CDCl_3$): δ = 13.48 (s, 1H); 8.74 (d, J = 15.2 Hz, 1H); 8.28 (d, J = 8.5 Hz, 1H); 8.00–7.82 (m, 4H); 7.72–7.64 (m, 1H); 7.61 (ddt, J = 8.3, 6.9, 1.4 Hz, 1H); 7.58–7.46 (m, 2H); 6.50 (ddd, J = 4.6, 2.5, 1.3 Hz, 2H); 3.87 (d, J = 1.2 Hz, 3H). ^{13}C NMR (126 MHz, $CDCl_3$): δ = 191.7, 166.8, 166.3, 141.4, 133.7, 132.3, 131.8, 131.3, 130.9, 128.8, 127.0, 126.3, 125.4, 125.2, 123.5, 123.0, 114.1, 107.8, 101.1, 55.6. HRMS (ESI-FT-ICR) *m/z*: 327.1000 [M + Na]; calcd. for $C_{20}H_{16}NaO_3$: 327.0997.

*5.2.5. (E)-1-(5-chloro-2-hydroxyphenyl)-3-(naphthalen-1-yl)prop-2-en-1-one (**5**)*

Yellow crystalline solid (88%), mp 165–165 °C. IR (cm^{-1}): 1642, 1556, 1462, 1403, 1365, 1358, 1332, 1327, 1275, 1242, 1207, 1190, 1024, 1013, 984, 826. ^{1}H NMR (500 MHz, $CDCl_3$): δ = 12.77 (s, 1H); 8.82 (d, J = 15.1 Hz, 1H); 8.28 (d, J = 8.9 Hz, 1H); 8.02–7.94 (m, 2H); 7.92 (dt, J = 3.4, 1.9 Hz, 2H); 7.72–7.60 (m, 2H); 7.60–7.50 (m, 2H); 7.46 (dd, J = 8.9, 2.5 Hz, 1H); 7.02 (d, J = 8.9 Hz, 1H). ^{13}C NMR (126 MHz, $CDCl_3$): δ = 192.7, 162.2, 143.4, 136.3, 133.8, 131.8, 131.7, 131.6, 128.9, 128.9, 127.3, 126.5, 125.6, 125.4, 123.6, 123.3, 122.0, 120.6, 120.3. HRMS (ESI-FT-ICR) *m/z*: 307.0522 [M − H]; calcd. for $C_{19}{}^{35}ClH_{12}O_2$: 307.0526; *m/z*: 309.0499 [M − H]; calcd. for $C_{19}{}^{37}ClH_{12}O_2$: 309.0496.

*5.2.6. (E)-1-(5-benzyloxy)-2-hydroxyphenyl)-3-(naphthalen-1-yl)prop-2-en-1-one (**6**)*

Orange crystalline solid (76%), mp 140–141 °C. IR (cm^{-1}): 1637, 1566, 1486, 1415, 1358, 1339, 1327, 1282, 1235, 1214, 1192, 1176, 1013, 965, 849, 837. ^{1}H NMR (500 MHz, $CDCl_3$): δ = 12.41 (s, 1H); 8.76 (d, J = 15.2 Hz, 1H); 8.27 (d, J = 8.4 Hz, 1H); 7.97 (d, J = 8.2 Hz, 1H); 7.90 (dd, J = 13.9, 7.6 Hz, 2H); 7.67–7.51 (m, 4H); 7.51–7.30 (m, 6H); 7.23 (dd, J = 9.1, 2.9 Hz, 1H); 7.00 (d, J = 9.0 Hz, 1H); 5.08 (s, 2H). ^{13}C NMR (126 MHz, $CDCl_3$): δ = 193.2, 158.2, 150.9, 142.4, 136.8, 133.8, 132.1, 131.8, 131.3, 128.8, 128.7, 128.2, 127.6, 127.2, 126.4, 125.4, 125.3, 125.0, 123.4, 122.8, 119.6, 119.4, 114.6, 71.3. HRMS (ESI-FT-ICR) *m/z*: 403.1314 [M + Na]; calcd. for $C_{26}H_{20}NaO_3$: 403.1310.

*5.2.7. (E)-1-(4-benzyloxy)-2-hydroxyphenyl)-3-(naphthalen-1-yl)prop-2-en-1-one (**7**)*

Yellow amorphous solid (60%). IR (cm^{-1}): 1633, 1566, 1507, 1363, 1289, 1254, 1218, 1190, 1128, 1020, 970, 830. ^{1}H NMR (500 MHz, $CDCl_3$): δ = 13.45 (s, 1H); 8.75 (d, J = 15.2 Hz, 1H); 8.28 (d, J = 8.5 Hz, 1H); 7.98–7.84 (m, 4H); 7.67 (d, J = 15.2 Hz, 1H); 7.64–7.49 (m, 3H); 7.49–7.32 (m, 5H); 6.64–6.53 (m, 2H); 5.13 (s, 2H). ^{13}C NMR (126 MHz, $CDCl_3$): δ = 191.7, 166.7, 165.4, 141.4, 135.8, 133.7, 132.3, 131.8, 131.4, 130.9, 128.8, 128.7, 128.3, 127.6, 127.0, 126.4, 125.4, 125.2, 123.5, 123.0, 114.3, 108.3, 102.1, 70.3. HRMS (ESI-FT-ICR) *m/z*: 403.1007 [M + Na]; calcd. for $C_{26}H_{20}NaO_3$: 403.1310.

*5.2.8. (E)-1-(3,5-dichloro-2-hydroxyphenyl)-3-(naphthalen-1-yl)prop-2-en-1-one (**8**)*

Orange crystalline solid (83%), mp 188–189 °C. IR (cm^{-1}): 1633, 1557, 1436, 1339, 1320, 1271, 1240, 1211, 1166, 1128, 1048, 1029, 975, 968, 866, 844, 821. ^{1}H NMR (500 MHz, $CDCl_3$): δ = 13.41 (s, 1H); 8.87 (d, J = 15.1 Hz, 1H); 8.27 (dd, J = 8.5, 1.1 Hz, 1H); 8.03–7.94 (m, 2H); 7.92 (dd, J = 8.5, 1.2 Hz, 1H); 7.85 (d, J = 2.5 Hz, 1H); 7.69–7.60 (m, 3H); 7.60–7.52 (m, 2H). ^{13}C NMR (126 MHz, $CDCl_3$): δ = 192.4, 158.1, 144.4, 135.8, 133.8, 132.0, 131.8, 131.4, 128.9, 127.5, 127.4, 126.5, 125.7, 125.4, 124.2, 123.3, 123.2, 121.3, 121.0. HRMS (ESI-FT-ICR) *m/z*: 341.0136 [M − H]; calcd. for $C_{19}{}^{35}Cl_2H_{11}O_2$: 341.0136; *m/z*: 343.0121 [M − H]; calcd. for $C_{19}{}^{35}Cl^{37}Cl\ H_{11}O_2$: 343.0107.

*5.2.9. (E)-1-(3,4-bis(benzyloxy)-2-hydroxyphenyl)-3-(naphthalen-1-yl) prop-2-en-1-one (**9**)*

Yellow amorphous solid (54%). IR (cm^{-1}): 1635, 1564, 1500, 1453, 1431, 1342, 1306, 1294, 1259, 1228, 1128, 1091, 1060, 1017, 986, 972. ^{1}H NMR (500 MHz, $CDCl_3$): δ = 13.28 (s, 1H); 8.75 (d, J = 15.2 Hz, 1H); 8.28 (d, J = 8.4 Hz, 1H); 7.94 (d, J = 8.2 Hz, 1H); 7.92–7.87 (m, 2H); 7.71–7.64 (m, 2H); 7.61 (ddd, J = 8.4, 6.8, 1.5 Hz, 1H); 7.58–7.49 (m, 4H); 7.42–7.28 (m, 8H); 6.55 (d, J = 9.1 Hz, 1H); 5.20 (s, 2H); 5.17 (s, 2H). ^{13}C NMR (126 MHz, $CDCl_3$): δ = 206.9, 192.3, 158.9, 158.0, 141.6, 137.6, 136.2, 133.7, 132.3, 131.8, 131.0, 128.8, 128.6, 128.6, 128.2, 128.1, 127.9, 127.2, 127.1, 126.4, 126.1, 125.4, 125.2, 123.5, 123.0, 115.7, 104.6, 74.8, 70.8. HRMS (ESI-FT-ICR) *m/z*: 509.1727 [M + Na]; calcd. for $C_{33}H_{26}NaO_4$: 509.1729.

*5.2.10. (E)-1-(2-(benzyloxy)-6-hydroxyphenyl)-3-(naphthalen-1-yl)prop-2-en-1-one (**10**)*

Bright yellow crystalline solid (80%), mp 145–146 °C. IR (cm^{-1}): 1630, 1555, 1460, 1446, 1353, 1233, 1209, 1169, 1065, 1024, 968, 918, 849. ^{1}H NMR (500 MHz, $CDCl_3$): δ = 13.41 (s, 1H); 8.62 (d, J = 15.4 Hz, 1H); 8.25 (dd, J = 8.5, 1.2 Hz, 1H); 7.95 (d, J = 15.4 Hz, 1H); 7.88–7.80 (m, 2H); 7.58–7.49 (m, 2H); 7.49–7.44 (m, 2H); 7.40 (t, J = 8.4 Hz, 1H); 7.38–7.34 (m, 1H); 7.32–7.27 (m, 2H); 7.21 (dd, J = 8.2, 7.2 Hz, 1H); 7.08 (dt, J = 7.2, 0.9 Hz, 1H); 6.68 (dd, J = 8.4, 1.0 Hz, 1H); 6.56 (dd, J = 8.3, 1.0 Hz, 1H); 5.14 (s, 2H). ^{13}C NMR (126 MHz, $CDCl_3$): δ = 194.5, 165.3, 160.3, 139.6, 136.0, 135.6, 133.6, 132.2, 131.8, 130.3, 130.0, 128.8, 128.6, 128.5, 128.5, 126.8, 126.1, 125.5, 125.0, 123.4, 112.0, 111.3, 102.4, 71.4. HRMS (ESI-FT-ICR) *m/z*: 403.1302 [M + Na]; calcd. for $C_{26}H_{20}NaO_3$: 403.1310.

*5.3. General procedure for the synthesis of flavanones (**11**–**19**)*

To a solution of a chalcone (0.12–0.2 mmol) in ethanol (1–2 mL), sodium acetate (10 equiv.) was added. The reaction was heated in refluxing for 24–48 h and then was allowed to cool to room temperature, poured into ice water (10 mL) and extracted with CH_2Cl_2 (3 × 5 mL). The combined organic phase was washed with brine, dried over Na_2SO_4, and then concentrated in vacuo. The flavanones were purified by crystallization (MeOH) or column chromatography.

*5.3.1. 2-(naphthalen-1-yl)chroman-4-one (**11**)*

Bright yellow crystalline solid (80%), mp 74–75 °C. IR (cm^{-1}): 1678, 1607, 1581, 1474, 1465, 1410, 1339, 1304, 1226, 1147, 1117, 1067, 1027, 984, 918, 901, 856, 840. ^{1}H NMR (500 MHz, $CDCl_3$): δ = 8.11–8.03 (m, 1H); 8.01 (dd, J = 8.0, 1.8 Hz, 1H); 7.97–7.86 (m, 2H); 7.79 (d, J = 7.1 Hz, 1H); 7.56 (m, 4H); 7.16–7.05 (m, 2H); 6.24 (dd, J = 13.4, 2.8 Hz, 1H); 3.28 (dd, J = 17.0, 13.4 Hz, 1H); 3.11 (dd, J = 17.0, 2.8 Hz, 1H). ^{13}C NMR (126 MHz, $CDCl_3$): δ = 192.3, 161.9, 136.3, 134.3, 134.0, 130.3, 129.5, 129.2, 127.3, 126.8, 126.1, 125.5, 124.0, 122.9, 121.9, 121.2, 118.3, 77.0, 44.1. HRMS (ESI-FT-ICR) *m/z*: 297.0901 [M + Na]; calcd. for $C_{19}H_{14}NaO_2$: 297.0891.

*5.3.2. 6-methyl-2-(naphthalen-1-yl)chroman-4-one (**12**)*

White crystalline solid (42%), mp 137–138 °C. IR (cm^{-1}): 1687, 1618, 1488, 1417, 1292, 1228, 1181, 1131, 1048, 982, 908. ^{1}H NMR (500 MHz, $CDCl_3$): δ = 8.09–8.02 (m, 1H); 7.96–7.85 (m, 2H); 7.83–7.75 (m, 2H); 7.62–7.47 (m, 3H); 7.35 (dd, J = 8.4, 2.4 Hz, 1H);

7.00 (d, J = 8.4 Hz, 1H); 6.20 (dd, J = 13.3, 2.8 Hz, 1H); 3.25 (dd, J = 17.0, 13.4 Hz, 1H); 3.08 (dd, J = 16.9, 2.9 Hz, 1H); 2.36 (s, 3H). ^{13}C NMR (126 MHz, $CDCl_3$): δ = 192.5, 159.9, 137.3, 134.3, 133.9, 131.2, 130.2, 129.3, 129.1, 126.7, 126.7, 125.9, 125.4, 123.8, 122.8, 120.7, 118.0, 76.8, 44.0, 20.5. HRMS (ESI-FT-ICR) m/z: 311.1049 [M + Na]; calcd. for $C_{20}H_{16}NaO_2$: 311.1048.

5.3.3. 6-methoxy-2-(naphthalen-1-yl)chroman-4-one ***(13)***

White crystalline solid (70%); mp 164–165 °C. IR (cm^{-1}): 1682, 1611, 1484, 1429, 1334, 1278, 1209, 1178, 1057, 1027, 982, 892, 866, 818. 1H NMR (500 MHz, $CDCl_3$): δ = 8.06 (d, J = 8.0 Hz, 1H); 7.92 (d, J = 8.4 Hz, 1H); 7.89 (d, J = 8.1 Hz, 1H); 7.78 (d, J = 7.1 Hz, 1H); 7.55 (m, 3H); 7.43 (d, J = 3.2 Hz, 1H); 7.15 (dd, J = 9.0, 3.2 Hz, 1H); 7.04 (d, J = 9.0 Hz, 1H); 6.19 (dd, J = 13.4, 2.8 Hz, 1H); 3.85 (s, 3H); 3.25 (dd, J = 17.1, 13.4 Hz, 1H); 3.09 (dd, J = 17.0, 2.8 Hz, 1H); ^{13}C NMR (126 MHz, $CDCl_3$): δ = 192.3, 156.5, 154.4, 134.3, 133.9, 130.2, 129.3, 129.1, 126.7, 125.9, 125.4, 125.4, 123.8, 122.8, 120.9, 119.5, 107.5, 77.2, 55.9, 43.9. HRMS (ESI-FT-ICR) m/z: 327.0999 [M + Na]; calcd. for $C_{20}H_{16}NaO_3$: 327.0997.

5.3.4. 7-methoxy-2-(naphthalen-1-yl)chroman-4-one ***(14)***

White amorphous solid (48%). IR (cm^{-1}): 1697, 1671, 1611, 1600, 1578, 1443, 1379, 1360, 1292, 1259, 1202, 1159, 1121, 1053, 1041, 1013, 991, 949, 892, 873, 828. ^{1}H NMR (500 MHz, $CDCl_3$): δ = 8.11–8.03 (m, 1H); 7.98–7.85 (m, 3H); 7.77 (d, J = 7.2 Hz, 1H); 7.55 (dd, J = 8.5, 6.6 Hz, 3H); 6.67 (dd, J = 8.8, 2.4 Hz, 1H); 6.54 (d, J = 2.4 Hz, 1H); 6.23 (dd, J = 13.3, 2.9 Hz, 1H); 3.85 (s, 3H); 3.23 (dd, J = 16.9, 13.3 Hz, 1H); 3.04 (dd, J = 17.0, 2.9 Hz, 1H). ^{13}C NMR (126 MHz, $CDCl_3$): δ = 190.9, 166.2, 163.7, 134.2, 133.9, 130.2, 129.4, 129.1, 128.9, 126.7, 126.0, 125.4, 123.9, 122.8, 115.0, 110.4, 101.0, 77.2, 55.7, 43.6. HRMS (ESI-FT-ICR) m/z: 327.1007 [M + Na]; calcd. for $C_{20}H_{16}NaO_3$: 327.0997.

5.3.5. 6-chloro-2-(naphthalen-1-yl)chroman-4-one ***(15)***

Bright yellow crystalline solid (80%), mp 137–138 °C; IR (cm^{-1}): 1687, 1604, 1467, 1424, 1408, 1337, 1275, 1221, 1209, 1171, 1131, 982, 911, 901, 892, 852, 833. ^{1}H NMR (500 MHz, $CDCl_3$) δ 8.06–8.00 (m, 1H); 7.96 (d, J = 2.6 Hz, 1H); 7.95–7.87 (m, 2H); 7.76 (dt, J = 7.3, 1.0 Hz, 1H); 7.61–7.51 (m, 3H); 7.48 (dd, J = 8.8, 2.7 Hz, 1H); 7.06 (d, J = 8.8 Hz, 1H); 6.23 (dd, J = 13.2, 2.9 Hz, 1H); 3.26 (dd, J = 17.1, 13.2 Hz, 1H); 3.12 (dd, J = 17.1, 2.9 Hz, 1H). ^{13}C NMR (126 MHz, $CDCl_3$) δ 191.2, 160.3, 136.2, 134.0, 133.8, 130.3, 129.7, 129.3, 127.5, 126.9, 126.6, 126.2, 125.5, 124.0, 122.8, 122.0, 120.1, 77.2, 43.7. HRMS (ESI-FT-ICR) m/z: 331.0505 [M + Na]; calcd. for $C_{19}{}^{35}ClH_{13}NaO_2$: 331.0502; m/z: 333.0463 [M + Na]; calcd. for $C_{19}{}^{37}ClH_{13}NaO_2$: 333.0472

5.3.6. 6-benzyloxy-2-(naphthalen-1-yl)chroman-4-one ***(16)***

White crystalline solid (46%), mp 159–160 °C. IR (cm^{-1}): 1682, 1484, 1453, 1431, 1382, 1337, 1271, 1181, 1155, 1131, 1062, 1039, 1027, 982, 963, 894, 861, 837. ^{1}H NMR (500 MHz, $CDCl_3$): δ = 8.05 (d, J = 7.8 Hz, 1H); 7.97–7.83 (m, 2H); 7.78 (d, J = 7.1 Hz, 1H); 7.61–7.50 (m, 4H); 7.46 (d, J = 7.4 Hz, 2H); 7.41 (dd, J = 8.4, 6.6 Hz, 2H); 7.37–7.29 (m, 1H); 7.23 (dd, J = 9.0, 3.2 Hz, 1H); 7.05 (d, J = 8.9 Hz, 1H); 6.19 (dd, J = 13.5, 2.8 Hz, 1H); 5.10 (s, 2H); 3.25 (dd, J = 17.1, 13.5 Hz, 1H); 3.09 (dd, J = 17.1, 2.8 Hz, 1H). ^{13}C NMR (126 MHz, $CDCl_3$): δ = 192.2, 156.6, 153.5, 136.6, 134.2, 133.9, 130.2, 129.3, 129.1, 128.6, 128.1, 127.6, 126.7, 126.0, 126.0, 125.4, 123.8, 122.8, 121.0, 119.6, 109.0, 77.0, 70.6, 43.9. HRMS (ESI-FT-ICR) m/z: 403.1310 [M + Na]; calcd. for $C_{26}H_{20}NaO_3$: 403.1310.

5.3.7. 7-benzyloxy-2-(naphthalen-1-yl)chroman-4-one ***(17)***

Pale yellow amorphous solid (50%). IR (cm^{-1}): 1668, 1607, 1571, 1500, 1443, 1377, 1353, 1334, 1294, 1252, 1185, 1166, 1119, 1060, 1034, 998, 984, 930, 828. 1H NMR (500 MHz, $CDCl_3$): δ = 7.98 (d, J = 7.7 Hz, 1H); 7.90–7.79 (m, 3H); 7.72–7.66 (m, 1H); 7.52–7.43 (m, 3H); 7.37–7.25 (m, 5H); 6.67 (dd, J = 8.8, 2.4 Hz, 1H); 6.55 (d, J = 2.3 Hz, 1H); 6.15 (dd, J = 13.2, 2.8 Hz, 1H); 5.04 (s, 2H); 3.16 (dd, J = 17.0, 13.3 Hz, 1H); 2.97 (dd, J = 17.0, 2.9 Hz, 1H). ^{13}C NMR (126 MHz, $CDCl_3$): δ = 190.8, 165.3, 163.7, 135.8, 134.2, 133.9, 130.2, 129.4, 129.1, 128.9, 128.7, 128.3, 127.5, 126.7, 126.0, 125.4, 123.9, 122.8, 115.2, 110.9, 102.0, 77.3, 70.3, 43.6. HRMS (ESI-FT-ICR) m/z: 403.1313 [M + Na]; calcd. for $C_{26}H_{20}NaO_3$: 403.1310.

5.3.8. 6,8-dichloro-2-(naphthalen-1-yl)chroman-4-one ***(18)***

Pale yellow crystalline solid (56%), mp 172–173 °C. IR (cm^{-1}): 1694, 1592, 1455, 1337, 1266, 1254, 1233, 1214, 1181, 1166, 1003, 982, 968, 878, 852, 809. ^{1}H NMR (500 MHz, $CDCl_3$): δ = 7.96 (d, J = 8.2 Hz, 1H); 7.89–7.82 (m, 2H); 7.80 (d, J = 2.6 Hz, 1H); 7.71 (d, J = 7.2 Hz, 1H); 7.56–7.44 (m, 4H); 6.23 (dd, J = 12.2, 3.5 Hz, 1H); 3.20 (dd, J = 17.2, 12.2 Hz, 1H); 3.13 (dd, J = 17.2, 3.5 Hz, 1H). ^{13}C NMR (126 MHz, $CDCl_3$): δ = 190.3, 155.9, 135.7, 133.9, 133.0, 130.1, 129.7, 129.1, 126.9, 126.8, 126.1, 125.3, 125.2, 124.4, 123.9, 122.7, 122.6, 77.6, 43.2. HRMS (ESI-FT-ICR) m/z: 365.0109 [M + Na]; calcd. for $C_{19}{}^{35}Cl_2H_{12}O_2$: 365.0112; m/z: 367.0089 [M + Na]; calcd. for $C_{19}{}^{35}Cl^{37}ClNaH_{12}O_2$: 367.0083

5.3.9. 7,8-bis(benzyloxy-2-(naphthalen-1-yl)chroman-4-one ***(19)***

White amorphous solid (40%). IR (cm^{-1}): 1686, 1641, 1592, 1505, 1446, 1384, 1312, 1293, 1261, 1194, 1120, 1090, 1073, 1013. 1H NMR (500 MHz, $CDCl_3$): δ = 8.05 (dd, J = 6.1, 3.3 Hz, 1H); 7.93 (dd, J = 6.3, 3.4 Hz, 1H); 7.90 (d, J = 8.3 Hz, 1H); 7.77 (d, J = 7.2 Hz, 1H); 7.73 (d, J = 8.9 Hz, 1H); 7.59–7.49 (m, 3H); 7.45–7.31 (m, 5H); 7.27 (m, 2H); 7.18 (dd, J = 8.4, 6.3 Hz, 1H); 7.15–7.06 (m, 2H); 6.74 (d, J = 8.9 Hz, 1H); 6.14 (dd, J = 12.3, 3.4 Hz, 1H); 5.21 (s, 2H); 5.01 (s, 2H); 3.16 (dd, J = 17.1, 12.3 Hz, 1H); 3.08 (dd, J = 17.0, 3.4 Hz, 1H). ^{13}C NMR (126 MHz, $CDCl_3$): δ = 205.9, 190.2, 157.3, 155.0, 136.2, 135.3, 135.1, 133.3, 132.7, 129.1, 128.1, 128.0, 127.6, 127.5, 127.1, 127.0, 126.8, 126.2, 125.6, 124.9, 124.3, 122.7, 122.0, 121.8, 115.4, 106.5, 74.2, 69.9, 42.8. HRMS (ESI-FT-ICR) m/z: 509.1729 [M + Na]; calcd. for $C_{33}H_{26}NaO_4$: 509.1732.

5.4. Cell culture and cytotoxicity assays

U-937, HL-60, NALM-6 and MOLT-3 cells were from DSMZ (German Collection of Microorganisms and Cell Cultures, Braunschweig, Germany). U-937/Bcl-2 cells were kindly provided by Dr. Jacqueline Bréard (INSERM U749, Faculté de Pharmacie Paris-Sud, Châtenay-Malabry, France). The U-937 is a pro-monocytic, human myeloid leukaemia cell line which was isolated from a histiocytic lymphoma. HL-60 is an acute myeloid leukaemia cell line. NALM-6 is a human B cell precursor leukaemia. MOLT-3 is an acute lymphoblastic leukaemia cell line.

Cells were cultured in RPMI 1640 medium containing 10% (v/v) heat-inactivated fetal bovine serum, 100 µg/ml streptomycin and 100 U/ml penicillin, incubated at 37 °C in a humidified atmosphere containing 5% CO_2 as described [17]. The doubling times of the cell lines were 30 h for U-937 and U-937/Bcl-2, 24 h for HL-60 and 40 h for NALM-6 and MOLT-3. Human peripheral blood mononuclear cells (PBMC) were isolated from heparin-anticoagulated blood of healthy volunteers by centrifugation with Ficoll-Paque Plus (GE Healthcare Bio-Sciences AB, Uppsala, Sweden). PBMC were also stimulated with phytohemagglutinine (2 µg/mL) for 48 h before the experimental treatment. The trypan blue exclusion method was used for counting the cells by a hematocytometer and the viability was always greater than 95% in all experiments. The cytotoxicities of chalcones and flavanones were evaluated by colorimetric 3-(4,5-dimethyl-2-thiazolyl-)-2,5-diphenyl-2*H*-tetrazolium bromide (MTT) assays as previously described [34]. Chalcones and flavanones were dissolved in DMSO and kept under dark conditions at 25 °C. Before each experiment, compounds were dissolved in culture media at 37 °C. The final concentration of DMSO did not exceed 0.3% (v/v).

5.5. Fluorescent microscopy analysis

Cells were washed with PBS and fixed in 3% paraformaldehyde for 10 min at room temperature. The paraformaldehyde was removed by centrifugation (12,000*g*, 1 min, 25 °C) and the samples were stained with 20 μg/mL of bisbenzimide trihydrochloride (Hoechst 33258) in PBS at 25 °C during 15 min. An aliquot of 10 μL of the mixture was used to observe the stained nuclei with fluorescent microscopy (Zeiss-Axiovert).

5.6. Quantification of hypodiploid cells and flow cytometry analysis of annexin V-FITC and propidium iodide-stained cells

Flow cytometric analysis of propidium iodide-stained cells was performed as previously described [35]. Briefly, cells were centrifuged for 10 min at 500*g*, washed with cold PBS, fixed with ice-cold 75% ethanol and stored at −20 °C for at least 1 h. Samples were then centrifuged at 500*g* for 10 min at 4 °C, washed with PBS, resuspended in 200 μL of PBS containing 100 μg/mL RNase A and 50 μg/mL propidium iodide and incubated for 1 h in the dark. The DNA content was analyzed by flow cytometry with a BD FACSVerse™ cytometer (BD Biosciences, San Jose, CA, USA). Flow cytometric analysis of annexin V-FITC and propidium iodide-stained cells was performed as described [35].

5.7. Assay of caspase activity

Caspase activity was determined by measuring proteolytic cleavage of the chromogenic substrates Ac-DEVD-*p*NA (for caspase-3 like protease activity), Ac-IETD-*p*NA (for caspase-8 activity) and Ac-LEHD-*p*NA (for caspase-9 activity) as previously described [35].

5.8. Western blot analysis

Cells were harvested by centrifugation (500*g*, 10 min, 4 °C) and pellets were resuspended in lysis buffer [1% Triton X-100, 10 mM sodium fluoride, 2 mM EDTA, 20 mM Tris-HCl (pH 7.4), 2 mM tetrasodium pyrophosphate, 10% glycerol, 137 mM NaCl, 20 mM sodium β-glycerophosphate], with the protease inhibitors phenylmethylsulfonyl fluoride (PMSF, 1 mM), aprotinin, leupeptin, and pepstatin A (5 μg/mL each) and kept on ice during 15 min. Cells were sonicated on ice five times (5 s each, with intervals between each sonication of 5 s) with a Braun Labsonic 2000 microtip sonifier and centrifuged (11,000*g*, 10 min, 4 °C). Bradford's method was used to determine protein concentration. The samples that were loaded in sodium dodecyl sulphate-polyacrylamide gel (from 7.5 to 15% depending on the molecular weight of interest) were prepared with the same amount of protein and boiled for 5 min. The proteins were transferred to a poly(vinylidene difluoride) membrane for 20 h at 20 V. The membrane was blocked with 10% nonfat milk in Tris-buffered saline [50 mM Tris-HCl (pH 7.4), 150 mM NaCl] containing 0.1% Tween-20 (TBST) for 1 h, followed by incubation with specific antibodies against caspase-3, caspase-4, caspase-6, caspase-7, caspase-8, caspase-9, Bax, Bcl-2, Bid, DR4, DR5, TRAIL, MAPKs, β-actin and poly(ADP-ribose)polymerase overnight at 4 °C. Membranes were washed three times with TBST and incubated for 1 h with the specific secondary antibody and the antigen-antibodies complexes were visualized by enhanced chemiluminescence using the manufacturer's protocol.

5.9. Subcellular fractionation

Cells were harvested by centrifugation (500*g*, 10 min, 4 °C) and washed twice with cold PBS at 4 °C. The pellets were resuspended in buffer [20 mM HEPES (pH 7.5), 1 mM EDTA, 0.1 mM phenylmethylsulfonyl fluoride, 1.5 mM $MgCl_2$, 1 mM EGTA, 10 mM KCl, 1 mM dithiothreitol, and 5 μg/mL leupeptin, aprotinin, and pepstatin A] with 250 mM sucrose. The samples were incubated for 15 min on ice and lysed 10 times with a 22-gauge needle. The lysates were centrifuged (1000*g*, 5 min, 4 °C). The supernatants were centrifuged at 105,000*g* for 45 min at 4 °C, and the resulting supernatant was used as the soluble cytosolic fraction and analysed by immunoblotting with specific antibodies against Smac/DIABLO and cytochrome *c*.

5.10. Intracellular reactive oxygen species (ROS) determination

Intracellular ROS were detected by flow cytometry using the probe 2′,7′-dichlorodihydrofluorescein diacetate (H_2-DCF-DA). Flow cytometric analysis was carried out using a BD FACSVerse™ cytometer (BD Biosciences, San Jose, CA, USA) and has been described in detail elsewhere [36].

5.11. Statistical methods

Statistical differences between means were tested using (i) Student's *t*-test (two samples) or (ii) one-way analysis of variance (ANOVA) (3 or more samples) with Tukey's test used for *a posteriori* pairwise comparisons of means. A significance level of $P < 0.05$ was used.

Acknowledgements

We thank Dr. Jacqueline Bréard (INSERM U749, Faculté de Pharmacie Paris-Sud., Châtenay-Malabry, France) for supplying U-937/Bcl-2 cells.

Funding

This work was supported in part by the Spanish Ministry of Science, Innovation and Universities and the European Regional Development Fund (PGC2018-094503-B-C21).

Conflict of interest

The authors declare that there is no conflict of interest.

Appendix A. Supplementary material

Supplementary data to this article can be found online at https://doi.org/10.1016/j.bioorg.2019.103450.

References

[1] R.L. Siegel, K.D. Miller, A. Jemal, Cancer statistics, 2018, CA Cancer J. Clin. 68 (2018) 7–30, https://doi.org/10.3322/caac.21442.
[2] F. Bray, J. Ferlay, I. Soerjomataram, R.L. Siegel, L.A. Torre, A. Jemal, Global cancer statistics GLOBOCAN estimates of incidence and mortality worldwide for 36 cancers in 185 countries, CA Cancer J. Clin. 68 (2018) (2018) 394–424, https://doi.org/10.3322/caac.21492.
[3] D.J. Newman, G.M. Cragg, Natural products as sources of new drugs from to 2014, J. Nat. Prod. 79 (2016) (1981) 629–661, https://doi.org/10.1021/acs.jnatprod.5b01055.
[4] D. Ravishankar, A.K. Rajora, F. Greco, H.M. Osborn, Flavonoids as prospective compounds for anti-cancer therapy, Int. J. Biochem. Cell Biol. 45 (2013) 2821–2831, https://doi.org/10.1016/j.biocel.2013.10.004.
[5] D. Raffa, B. Maggio, M.V. Raimondi, F. Plescia, G. Daidone, Recent discoveries of anticancer flavonoids, Eur. J. Med. Chem. 142 (2017) 213–228, https://doi.org/10.1016/j.ejmech.2017.07.034.
[6] S. Shalini, L. Dorstyn, S. Dawar, S. Kumar, Old, new and emerging functions of caspases, Cell Death Differ. 22 (2015) 526–539, https://doi.org/10.1038/cdd.2014.216.
[7] E.A. Meyer, R.K. Castellano, F. Diederich, Interactions with aromatic rings in chemical and biological recognition, Angew. Chem. Int. Ed. Engl. 42 (2003) 1210–1250, https://doi.org/10.1002/anie.200390319. Erratum. In: Angew Chem Int Ed Engl. 42 (2003) 4120.
[8] L.M. Salonen, M. Ellermann, F. Diederich, Aromatic rings in chemical and biological recognition: energetics and structures, Angew. Chem. Int. Ed. Engl. 50 (2011) 4808–4842, https://doi.org/10.1002/anie.201007560.
[9] J.L. Asensio, A. Ardá, F.J. Cañada, J. Jiménez-Barbero, Carbohydrate-aromatic interactions, Acc. Chem. Res. 46 (2013) 946–954, https://doi.org/10.1021/ar300024d.

[10] S. Makar, T. Saha, S.K. Singh, Naphthalene, a versatile platform in medicinal chemistry: sky-high perspective, Eur. J. Med. Chem. 161 (2019) 252–276, https://doi.org/10.1016/j.ejmech.2018.10.018.

[11] P. Harris, P. Ralph, Human leukemic models of myelomonocytic development: a review of the HL-60 and U937 cell lines, J. Leukoc. Biol. 37 (1985) 407–422, https://doi.org/10.1002/jlb.37.4.407.

[12] W. Chanput, V. Peters, H. Wichers, THP-1 and U937 cells, in: K. Verhoeckx, P. Cotter, I. López-Expósito, C. Kleiveland, T. Lea, A. Mackie, T. Requena, D. Swiatecka, H. Wichers (Eds.), The Impact of Food Bioactives on Health: *In Vitro* and *Ex Vivo* Models, Springer, 2015, pp. 147–159.

[13] B.M. Muller, J. Mai, R.A. Yocum, M.J. Adler, Impact of mono- and disubstitution on the colorimetric dynamic covalent switching chalcone/flavanone scaffold, Org. Biomol. Chem. 12 (2014) 5108–5114, https://doi.org/10.1039/C4OB00398E.

[14] A.A. Sy-Cordero, T.N. Graf, S.P. Runyon, M.C. Wani, D.J. Kroll, R. Agarwal, S.J. Brantley, M.F. Paine, S.J. Polyak, N.H. Oberlies, Enhanced bioactivity of silybin B methylation products, Bioorg. Med. Chem. 21 (2013) 742–747, https://doi.org/10.1016/j.bmc.2012.11.035.

[15] F. Grande, O.I. Parisi, R.A. Mordocco, C. Rocca, F. Puoci, L. Scrivano, A.M. Quintieri, P. Cantafio, S. Ferla, A. Brancale, C. Saturnino, M.C. Cerra, M.S. Sinicropi, T. Angelone, Quercetin derivatives as novel antihypertensive agents: synthesis and physiological characterization, Eur. J. Pharm. Sci. 82 (2016) 161–170, https://doi.org/10.1016/j.ejps.2015.11.021.

[16] M.K. Kim, K.S. Park, C. Lee, H.R. Park, H. Choo, Y. Chong, Enhanced stability and intracellular accumulation of quercetin by protection of the chemically or metabolically susceptible hydroxyl groups with a pivaloxymethyl (POM) promoiety, J. Med. Chem. 53 (2010) 8597–8607, https://doi.org/10.1021/jm101252m.

[17] E. Saavedra, H. Del Rosario, I. Brouard, J. Quintana, F. Estévez, 6'-Benzyloxy-4-bromo-2'-hydroxychalcone is cytotoxic against human leukaemia cells and induces caspase-8- and reactive oxygen species-dependent apoptosis, Chem. Biol. Interact. 298 (2019) 137–145, https://doi.org/10.1016/j.cbi.2018.12.010.

[18] J.A. Beutler, E. Hamel, A.J. Vlietinck, A. Haemers, P. Rajan, J.N. Roitman, J.H. Cardellina 2nd, M.R. Boyd, Structure-activity requirements for flavone cytotoxicity and binding to tubulin, J. Med. Chem. 41 (1998) 2333–2338, https://doi.org/10.1021/jm970842h.

[19] F. Estévez-Sarmiento, M. Said, I. Brouard, F. León, C. García, J. Quintana, F. Estévez, 3'-Hydroxy-3,4'-dimethoxyflavone blocks tubulin polymerization and is a potent apoptotic inducer in human SK-MEL-1 melanoma cells, Bioorg. Med. Chem. 25 (2017) 6060–6070, https://doi.org/10.1016/j.bmc.2017.09.043.

[20] S. Rubio, J. Quintana, J.L. Eiroa, J. Triana, F. Estévez, Betuletol 3-methyl ether induces G_2-M phase arrest and activates the sphingomyelin and MAPK pathways in human leukemia cells, Mol. Carcinog. 49 (2010) 32–43, https://doi.org/10.1002/mc.20574.

[21] F. Torres, J. Quintana, F. Estévez, 5,7,3'-trihydroxy-3,4'-dimethoxyflavone-induced cell death in human leukemia cells is dependent on caspases and activates the MAPK pathway, Mol. Carcinog. 49 (2010) 464–475, https://doi.org/10.1002/mc.20619.

[22] S. Inoue, G. Browne, G. Melino, G.M. Cohen, Ordering of caspases in cells undergoing apoptosis by the intrinsic pathway, Cell Death Differ. 16 (2009) 1053–1061, https://doi.org/10.1038/cdd.2009.29.

[23] O. Julien, J.A. Wells, Caspases and their substrates, Cell Death Differ. 24 (2017) 1380–1389, https://doi.org/10.1038/cdd.2017.44.

[24] D.C. Gray, S. Mahrus, J.A. Wells, Activation of specific apoptotic caspases with an engineered small-molecule-activated protease, Cell 142 (2010) 637–646, https://doi.org/10.1016/j.cell.2010.07.014.

[25] O. Julien, M. Zhuang, A.P. Wiita, A.J. O'Donoghue, G.M. Knudsen, C.S. Craik, J.A. Wells, Quantitative MS-based enzymology of caspases reveals distinct protein substrate specificities, hierarchies, and cellular roles, Proc. Natl. Acad. Sci. USA 113 (2016) E2001–E2010, https://doi.org/10.1073/pnas.1524900113.

[26] P. Li, D. Nijhawan, I. Budihardjo, S.M. Srinivasula, M. Ahmad, E.S. Alnemri, X. Wang, Cytochrome c and dATP-dependent formation of Apaf-1/caspase-9 complex initiates an apoptotic protease cascade, Cell 91 (1997) 479–489, https://doi.org/10.1016/s0092-8674(00)80434-1.

[27] G.S. Salvesen, C.S. Duckett, IAP proteins: blocking the road to death's door, Nat. Rev. Mol. Cell Biol. 3 (2002) 401–410, https://doi.org/10.1038/nrm830.

[28] R.W. Birkinshaw, P.E. Czabotar, The BCL-2 family of proteins and mitochondrial outer membrane permeabilisation, Semin. Cell Dev. Biol. 72 (2017) 152–162, https://doi.org/10.1016/j.semcdb.2017.04.001.

[29] Q. Peng, Z. Deng, H. Pan, L. Gu, O. Liu, Z. Tang, Mitogen-activated protein kinase signaling pathway in oral cancer, Oncol Lett. 15 (2018) 1379–1388, https://doi.org/10.3892/ol.2017.7491.

[30] Y. Sun, W.Z. Liu, T. Liu, X. Feng, N. Yang, H.F. Zhou, Signaling pathway of MAPK/ERK in cell proliferation, differentiation, migration, senescence and apoptosis, J. Recept. Signal Transduct. Res. 35 (2015) 600–604, https://doi.org/10.3109/10799893.2015.1030412.

[31] S. Rubio, J. Quintana, J.L. Eiroa, J. Triana, F. Estévez, Betuletol 3-methyl ether induces G(2)-M phase arrest and activates the sphingomyelin and MAPK pathways in human leukemia cells, Mol. Carcinog. 49 (2010) 32–43, https://doi.org/10.1002/mc.20574.

[32] F. Torres, J. Quintana, J.G. Díaz, A.J. Carmona, F. Estévez, Trifolin acetate-induced cell death in human leukemia cells is dependent on caspase-6 and activates the MAPK pathway, Apoptosis 13 (2008) 716–728, https://doi.org/10.1007/s10495-008-0202-0.

[33] D. Wang, Q. Sun, J. Wu, W. Wang, G. Yao, T. Li, X. Li, L. Li, Y. Zhang, W. Cui, S. Song, A new Prenylated Flavonoid induces G0/G1 arrest and apoptosis through p38/JNK MAPK pathways in Human Hepatocellular Carcinoma cells, Sci. Rep. 7 (2017) 5736, https://doi.org/10.1038/s41598-017-05955-0.

[34] T. Mosmann, Rapid colorimetric assay for cellular growth and survival: application to proliferation and cytotoxicity assays, J. Immunol. Methods 65 (1983) 55–63, https://doi.org/10.1016/0022-1759(83)90303-4.

[35] S. Estévez, M.T. Marrero, J. Quintana, F. Estévez, Eupatorin-induced cell death in human leukemia cells is dependent on caspases and activates the mitogen-activated protein kinase pathway, PLoS One 9 (2014) e112536, https://doi.org/10.1371/journal.pone.0112536.

[36] F. Estévez-Sarmiento, E. Hernández, I. Brouard, F. León, C. García, J. Quintana, F. Estévez, 3'-Hydroxy-3,4'-dimethoxyflavone-induced cell death in human leukaemia cells is dependent on caspases and reactive oxygen species and attenuated by the inhibition of JNK/SAPK, Chem. Biol. Interact. 288 (2018) 1–11, https://doi.org/10.1016/j.cbi.2018.04.006.